APPLICATION OF THYRISTOR-CONTROLLED SERIES REACTOR FOR FAULT CURRENT LIMITATION AND POWER SYSTEM STABILITY ENHANCEMENT

by

Bu Il Kang

Bachelor of Science, Chonnam National University, 1994

A thesis submitted to the

Faculty of the Graduate School of the

University of Colorado in partial fulfillment

of the requirements for the degree of

Master of Science

Electrical Engineering

2013

This thesis for the Master of Science degree by

Bu Il Kang

has been approved for the

Electrical Engineering Program

by

Jae-Do Park, Chair

Fernando Mancilla-David

Yiming Deng

April 16, 2013

Kang, Bu Il (M.S., Electrical Engineering)

Application of Thyristor-Controlled Series Reactor for Fault Current Limitation and Power System Stability Enhancement

Thesis directed by Assistant Professor Jae-Do Park.

ABSTRACT

Various types of Fault Current Limiters (FCLs) have been proposed and proven that they offer many advantages with respect to transmission losses, voltage quality, and power system stability. However, those including the Solid-State Fault Current Limiters (SSFCL), the most advanced type of FCL, have been mainly focusing on the FCL system itself such as optimization of components, improving the efficiency and reducing the cost. Conventional ways such as splitting buses, replacing the switchgear, and installing permanently-inserted series reactor are still used to avoid fault current problems, which impairs overall power system reliability. In this thesis, a Thyristor-Controlled Series Reactor (TCSR) is presented to limit the fault current and enhance the power system stability simultaneously. The influence of TCSR is analyzed from the perspective of voltage security enhancement and the feasibility of real power system application is assessed. The benefits of the TCSR are demonstrated with bulk power system simulation results from the voltage security and angle stability stand point.

The form and content of this abstract are approved. I recommend its publication.

Approved: Jae-Do Park

DEDICATION

I dedicate this work to Eungjeong, my lovely wife, who has always believed and supported me by my side.

ACKNOWLEDGMENTS

This thesis would not have been possible without the support of my company, Korea Power Exchange (KPX).

TABLE OF CONTENTS

CHAPTER

I. INTRODUCTION 1

Introduction 1

II. FAULT CURRENT LIMITERS 3

Fault Current Limitation by a Series Reactor 3

Bypass Switch 4

Tuned LC Circuit Shunted by a Metal Oxide Varistor (MOV) 5

Series Compensator 6

Power Electronic Switches 11

III. POWER SYSTEM STABILITY 13

Thyristor Controlled Series Compensator (TCSC) 17

Short Circuit Current Limiter (SCCL) 20

IV. D-Q TRANSFORMATION 22

V. PROPOSED APPROACH 29

Voltage Stabilizing Fault Current Limiter 29

Plant Model and Compensator Design 32

VI. COMPUTER SIMULATIONS 37

Duty Control to Increase Output Voltage 37

Effects of TCSR on Different Fault Locations 40

Effects of TCSR on Bulk Power System Voltage Stability 44

Effects of TCSR on Bulk Power System Angle Stability 46

VII. CONCLUSION 51

LIST OF TABLES

Table

VI.1 Simulation parameters 38

VI.2 Comparison results of the voltage and the fault current 45

VI.3 Fault current of the adjacent buses with respect to 4400 bus fault 48

VI.4 Fault current of critical buses(kA) 48

VI.5 Case summary(MW) 48

VI.6 Critical Clearing Time(msec) 48

LIST OF FIGURES

Figure

II.1 Fault current limiter application: it protects the entire bus or individual circuit..... 4

II.2 Relationship between system voltage drop, reactor short-circuit voltage and power factor. 5

II.3 Fault current limiter with tuned impedance. 6

II.4 Fault current limiter using a tuned LC circuit shunted by a MOV. 7

II.5 Power system network with SC. 8

II.6 Power system network during the source side fault with compensation..... 9

II.7 Network model and phasor diagram under the prefault condition. 10

II.8 Network model and phasor diagram under the load side fault condition..... 10

II.9 FCL using power electronic switches (a) Short Circuit Current Limiter (SCCL), (b) Solid-State Fault Current Limiter (SSFCL). 12

III.1 Shunt compensation with a current source (a) Network configuration, (b) Phasor diagram: V_R can be controlled V_R to V'_R by compensating the reactive component of the load current. 13

III.2 Series compensation with a voltage source (a) Network configuration, (b) Phasor diagram: V_R can be controlled by inserting V_{COMP} and the appropriate magnitude control of V_{COMP}. 14

III.3 Equivalent circuit of single-machine infinite bus system: a generator delivers power to an infinite bus through two transmission circuits. 17

III.4 Power-angel curve for Equal Area Criterion. 17

III.5 A practical configuration of TCSC. 18

III.6 Impedance characteristics of a TCSC with respect to firing angle. 19

III.7 The characteristics of SCCL and power-angle curve (a) During normal operation, equivalent impedance is treated as zero and XL during the fault (b) Accelerating power is decreased as much as the hatched area by inserting the series reactor. 20

IV.1 Axes of reference frame..... 23

IV.2 Voltage and current waveforms when duty ratio is 0 where the current flows only through the series reactor. (a) Load voltage (b) Current. 27

IV.3 Voltage and current waveforms when duty ratio is 1 where the current flows only through the bypass switch. (a) Load voltage (b) Current. 28

V.1 Model for circuit analysis (a) Original circuit, (b) Equivalent circuit when switch is off, (c) Equivalent circuit when switch is on. 30

V.2 PI regulator with negative feedback. 34

VI.1 Step responses of the plant: Uncompensated model has a steady state error (0.4651), which is eliminated by a PI controller where K_P=0.8, K_I=100. 38

VI.2 Overall model configuration and the output voltage responses: the output voltage changes from about 245kV to 270kV based on the duty ratio which starts to increase from 0.5sec. 39

VI.3 Typical power system model to investigate the effects of TCSR on fault currents and voltage dips: faults can be occurred either near the TCSR or far away from it. 40

VI.4 Simulation results for the fault near the TCSR: The TCSR is required to be operated as fault current limiter and voltage restorer. (a) The bus voltage is operating in low level when the series reactor is inserted. (b) The fault current is exceeding the nominal value when the series reactor is bypassed. (c) Voltage is maintained higher and the fault current is limited within nominal value when the control scheme is applied. 42

VI.5 Simulation results for the fault far away from the TCSR: The TCSR is required to be operated as voltage restorer. (a) The bus voltage is operating in low level when the series reactor is inserted. (b) The voltage is maintained higher and the fault current is in low level when the series reactor is bypassed. (c) Voltage is maintained higher and no control action is required to limit the fault current. 43

VI.6 A 345kV transmission network for the voltage stability simulation: three substation buses can be reconnected when the TCSR is installed. 44

VI.7 P-V curves during normal and contingent conditions: maximum incremental transfer is increased from 300MW to 475MW when the TCSR is used. 45

VI.8 Power angle curve for Equal Area Criterion: power system synchronism can be maintained when the accelerating power is smaller than the decelerating power and inserting the series reactor decreases the accelerating power as much as the hatched area. 46

VI.9 Network configuration for the transient stability simulation: a FCL using permanently-inserted series reactor is installed on a substation and two contingency cases (F1, F2) are studied to analyze the influences of the FCL on the power system angle stability. 47

VI.10 Simulation results on F1 fault: the power system can maintain synchronism with the TCSR (a) Machine electrical power [P.U.] (b) Bus voltage [P.U.]. 49

VI.11 Simulation results on F2 fault: the power system can maintain synchronism with the TCSR (a) Machine electrical power [P.U.] (b) Bus voltage [P.U.]. 50

LIST OF EQUATIONS

Equation

II.1 Equation for system voltage drop. 3

II.2 Equation for the current increase. 5

II.3 Equation for the receiving end voltage. 7

II.4 Circuit equations. 7

II.5 Injection voltage equation. 8

II.6 Current and voltage equations under the prefault condition. 9

II.7 Current and voltage equation during the fault. 9

III.1 Voltage equation for simple AC circuit. 15

III.2 Voltage equation for the series compensated AC system. 15

III.3 Relationship between the rotor angle and the accelerating power. 16

III.4 Equivalent impedance of TCSC 19

IV.1 Transformation matrix. 22

IV.2 Column vector and transformation matrix. 23

IV.3 Conversion variables in different reference frames. 24

IV.4 Conversion variables in the stationary reference frames. 24

IV.5 Conversion variables in the synchronous reference frames. 25

IV.6 Space vector represented by three-phase components 25

IV.7 Space vector in the stationary reference frame. 26

IV.8 Transformation to other reference frame. 26

IV.9 Individual variables f_a, f_b, f_c. 26

V.1 Voltage and current equations in case the thyristor switches are open. 29

V.2 Voltage and current equations in case the thyristor switches are close. 31

V.3 Averaged voltage and current dynamic equations. 32

V.4 Linearized function. 32

V.5 Dynamic model including steady-state term and linear small signal term. 33

V.6 Linearized small signal dynamic model..... 33

V.7 Control transfer functions. 34

V.8 Control transfer function for the plant model. 35

V.9 A PI compensator model. 35

V.10 Closed-loop transfer function..... 35

CHAPTER I

INTRODUCTION

Introduction

Demand on electricity has been increasing tremendously and many countries invest significant amount of money for reliable power supply. More generation plants and transmission lines were constructed and the power systems became more complex. Major transmission lines tend to be long-distance and generation sites are large-scaled. Load concentration requires more transmission lines to be interconnected. However, those characteristics of power systems have been causing problems related to fault currents and system stabilities.

Several approaches to cope with the fault current problems are being used in distribution and transmission areas. Permanently-inserted series reactors, up-rating and replacement of switchgear, splitting buses or transmission lines are the most commonly used techniques to limit the fault current in power systems, which are regarded as cost-effective and more secure measures for the operational reliability of power system facilities. However, up-rating and replacement of switchgear can be very expensive and short-circuit current duty may not be reduced. Network splitting can deteriorate the power system security. Permanently-inserted current-limiting series reactors introduce a voltage drop, active and reactive power losses and also adversely affect the power system stability. In spite of these drawbacks, a lot of power systems are still divided into several subsystems to solve fault current problems.

For the power system stability enhancement, on the other hand, the following has been used as countermeasures in general: (1) Constructing more interconnection lines, (2)

Installing dynamic reactive resources, (3) Constraining power transfers, and (4) Using Special Protection Schemes (SPS).

So far, fault current and stability analysis has been studied separately, since network configuration influences in an opposite way to those problems. When transmission systems are fully meshed, they tend to yield fault current problems, rather than stability problems. On the other hand, when powers are delivered through high impedance transmission lines, stability issues may arise instead of fault current problems. However, as the power systems become more complex with the meshed transmission networks which are interconnected with long-distance, high-power transfer transmission lines, those two problems become co-existent. Consequently, countermeasures to deal with the fault current impact more on the power system stability than before.

In this work, prior researches related to fault currents limitation and power system stability enhancement are reviewed and a TCSR that limits the fault current and improves the stability simultaneously is presented. The influence of the TCSR from the perspective of voltage security enhancement is shown with a theoretical analysis, and to assess the feasibility of the TCSR to real power systems, the benefits of the TCSR are demonstrated with bulk power system simulation results.

CHAPTER II

FAULT CURRENT LIMITERS

Fault current limiters can be applied in a variety of distribution and transmission areas. Those can be used for the protection of entire bus or individual circuit as in Figure II.1. For the last 20 years, super-conductive FCLs have been studied and suggested to limit the fault current, but they have not been used widely in the field because of the cost problem. Reactors, high impedance transformers, circuit breaker upgrades and splitting buses or transmission lines are still widely used. Because of the fault current problem, many power system operators are sacrificing their system reliability by splitting the network into many sub-systems. However, comparing to the Superconductive FCL, these methods have many disadvantages with respect to transmission losses and system reliability. Many alternative ways to overcome those problems have been suggested.

Fault Current Limitation by a Series Reactor

Most commonly used FCLs are permanently-inserted series reactor type fault current limiters. As this type of fault current limiter does not require replacement of switchgear and more economical than others, it is commonly used in power systems. The fault current driven by the voltage source is reduced by the impedance of the reactor.

$$\left|\frac{\Delta V}{V_N}\right| = 1 - \frac{1}{\sqrt{1 + 2V_k\sqrt{1 - \cos^2 \emptyset} + {V_k}^2}}$$

Equation II.1 Equation for system voltage drop.

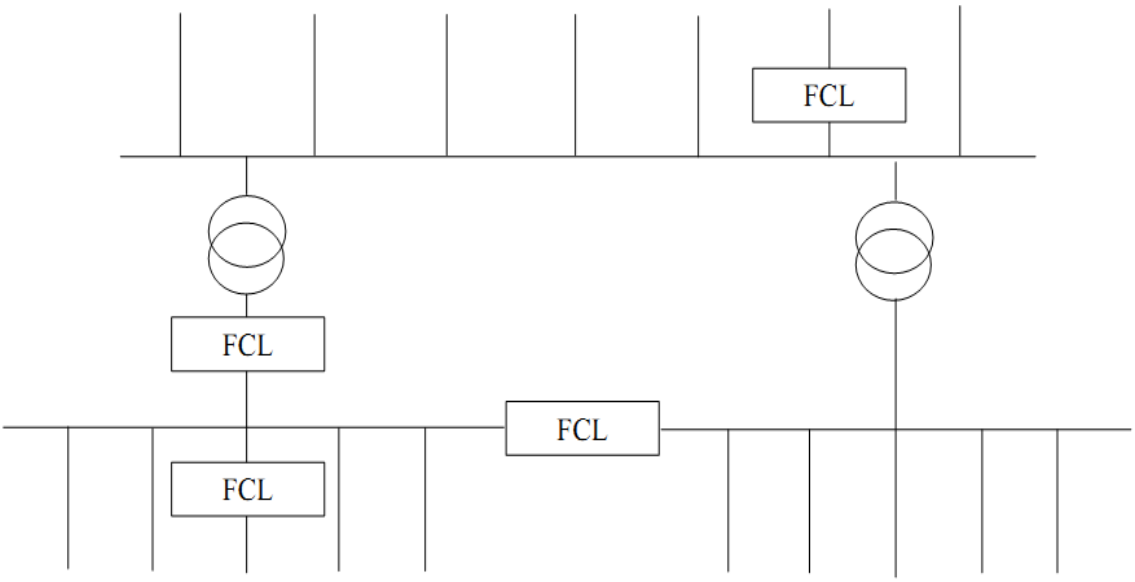

Figure II.1 Fault current limiter application: it protects the entire bus or individual circuit.

However, it may cause severe voltage drop during contingent state, while the system voltage drop may not represent a particular problem during normal operating conditions [1]. The system voltage drop can be calculated using the following equation and Figure II.2 shows the relationship between system voltage drop, reactor short-circuit voltage V_k, and power factor.

Bypass Switch

In the 1980s, most power systems were operating with splitting network topology such as splitting buses or opening transmission lines at normal operating conditions to limit the fault current. A tuned-circuit impedance method was proposed to limit the fault current by Electric Power Research Institute (EPRI) [2]. Figure II.3 shows the basic configuration of this circuit. Under normal operating conditions, the switch is opened and transmission line has zero net impedance if they are tuned properly. When a fault occurs, the switch is closed and the equivalent impedance becomes $\frac{X^2}{R}$ where X is the impedance

of the reactive components, which results in fault current reduction. Although it requires high initial cost, its zero net impedance during normal operating conditions can reduce the operating cost such as transmission loss; besides, the system voltage recovers to its prefault level after clearing the fault.

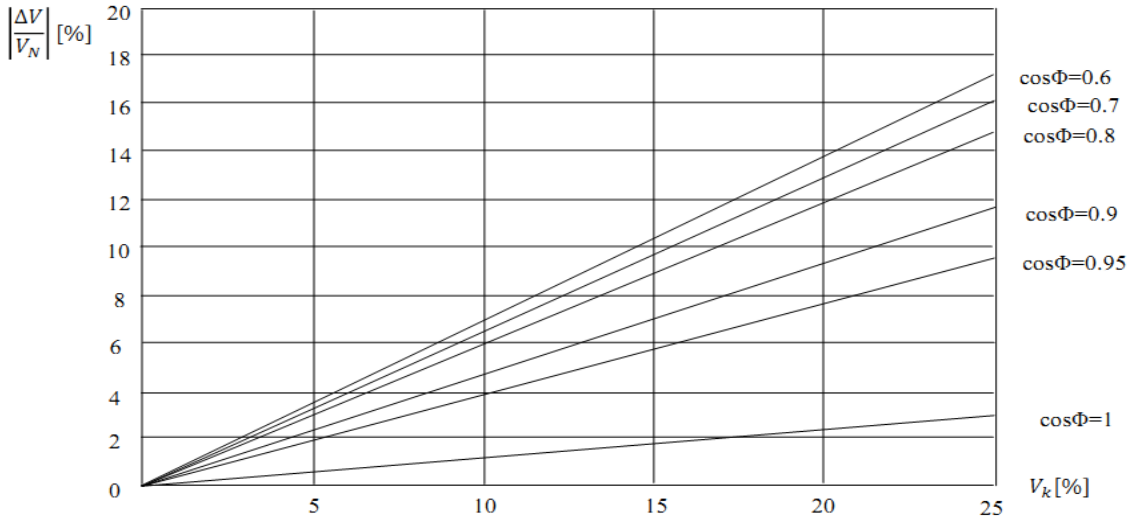

Figure II.2 Relationship between system voltage drop, reactor short-circuit voltage and power factor.

Tuned LC Circuit Shunted by a Metal Oxide Varistor (MOV)

This type of FCL was developed for the fault current limitation and power quality improvement [3]. It consists of a series LC circuit tuned at the system frequency and a MOV in parallel with the capacitor as shown in Figure II.4. Since the LC circuit is well-tuned, it is almost transparent during normal operation. When there is a fault in the downstream of the FCL, it forces a gradual increase of the current, which is justified by the following equations.

$$i(t) = V_P[\frac{1}{Z}\sin(wt + \theta - \delta) + \frac{1}{2wL}\sin\theta\sin wt + \frac{1}{2wL}wt\sin(wt + \theta)]$$

Equation II.2 Equation for the current increase.

Where, V_P: magnitude of the source voltage, Θ: phase angle of the source voltage, Z: the magnitude of the load impedance, δ: load angle.

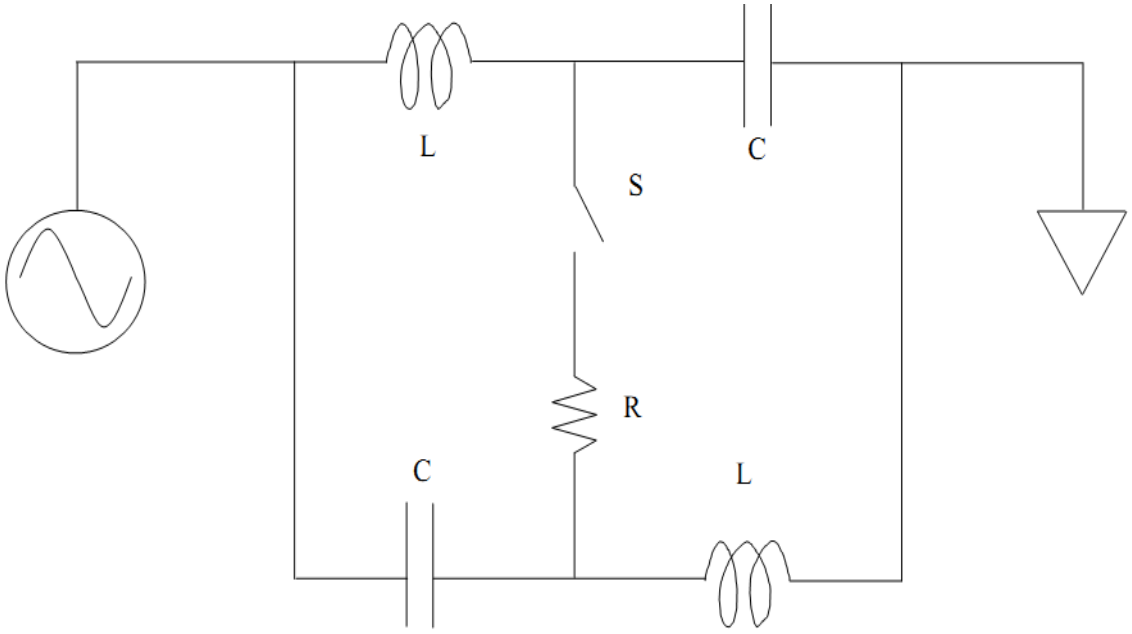

Figure II.3 Fault current limiter with tuned impedance.

This shows that the higher the L, the slower the current increase, which reduces the voltage sag during the fault. However, since the voltage on the L and C will increase during the fault, additional device to limit the over-voltage is required. MOV is connected in parallel with the capacitor, and it absorbs the excessive energy in case its protection level is reached. However, long cool-down time of the MOV and possibility of Sub-Synchronous Resonance (SSR) [4] are the drawback to be solved.

Series Compensator

Dynamic voltage restorer (DVR) using energy storage device and a series compensator (SC) shown in Figure II.5 was proposed to limit the fault current and improve the voltage quality of the power system [5, 6]. By controlling the amplitude and

phase angle, they control the real and reactive power between the controller and the power system.

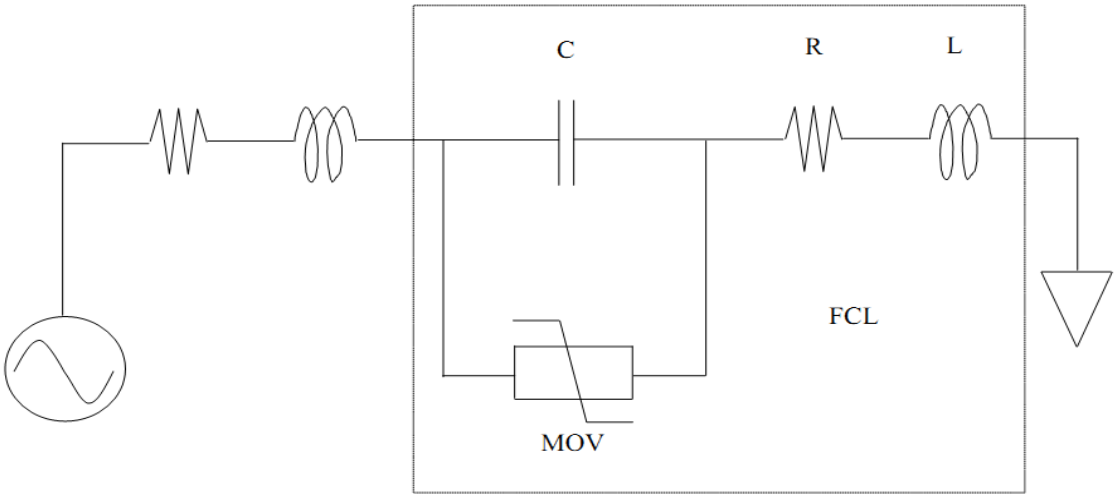

Figure II.4 Fault current limiter using a tuned LC circuit shunted by a MOV.

During normal operating conditions where the receiving end voltage V_L is given by

$$\overrightarrow{V_L} = \overrightarrow{V_S} - jX_S\overrightarrow{I_L}$$

Equation II.3 Equation for the receiving end voltage.

, the SC does not operate. However, when there is a fault in the network, it compensates the voltage by injecting a lagging or leading voltage in quadrature with the load (fault) current to restore the line voltage and limit the fault current. Considering a fault at the source side, the voltage of the source will be dropped, and the circuit equation becomes

$$\text{Without compensation}: \overrightarrow{V_{PF}} = \overrightarrow{V'_L} = \overrightarrow{V_{SAG}} - jX_S\overrightarrow{I'_L}$$

$$\text{With compensation}: \overrightarrow{V_L} = \overrightarrow{V_{SAG}} - jX_S\overrightarrow{I_L} + \overrightarrow{V_{SC}}$$

Equation II.4 Circuit equations.

Where $\overrightarrow{V'_L}, \overrightarrow{I'_L}$ and $\overrightarrow{V_{PF}}$ are the load side voltage, line current, and SC side voltage vector during the fault respectively.

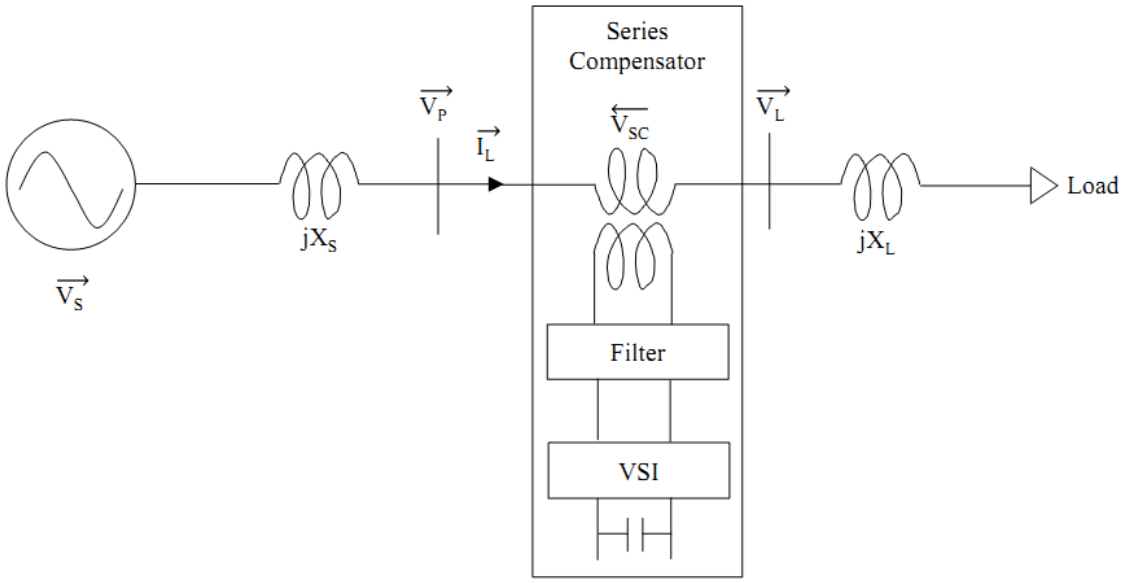

Figure II.5 Power system network with SC.

To enhance the voltage drop, the SC injects a lagging voltage $\overrightarrow{V_{SC}}$ until the load side voltage is restored to its prefault level $\overrightarrow{V_L}$ as shown in Figure II.6. Since $\overrightarrow{V_{SAG}} - jX_S\overrightarrow{I_L}$ is the voltage on the source side of the SC and if we set $\overrightarrow{V_L} = \overrightarrow{V_P}$, then the injection voltage $\overrightarrow{V_{SC}}$ becomes

$$\overrightarrow{V_{SC}} = \overrightarrow{V_P} - \overrightarrow{V'_{PF}}$$

Equation II.5 Injection voltage equation.

$\overrightarrow{V'_{PF}}$: measured voltage on the source side of the Series Compensator (SC). By injecting a lagging voltage, we allow the DVR to restore the load side voltage to its pre-defined

level under normal and contingency conditions. On the other hand, if the fault occurs at the load side, the SC should act as a fault current limiter.

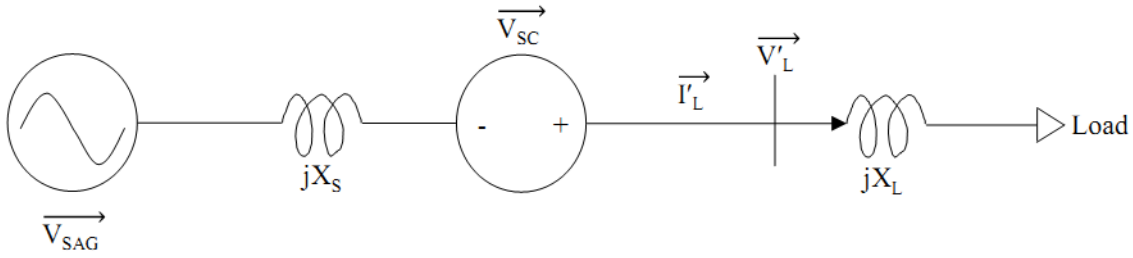

Figure II.6 Power system network during the source side fault with compensation.

The current and voltage equations under the prefault condition can be expressed as

$$\overrightarrow{V_S} - \overrightarrow{V_P} - jX_S\overrightarrow{I_L} = 0$$

$$\overrightarrow{V_P} - \overrightarrow{V_F} - jX\overrightarrow{I_L} = 0$$

$$\overrightarrow{I_L} = \frac{\overrightarrow{V_S} - \overrightarrow{V_P}}{jX_S}$$

Equation II.6 Current and voltage equations under the prefault condition.

, and the system model is shown in Figure II.7. During the fault where the $\overrightarrow{V_F}$ = 0, those equations become

$$\overrightarrow{V_S} - \overrightarrow{V_{PF}} - jX_S\overrightarrow{I_L} = 0$$

$$\overrightarrow{V_{PF}} - jX\overrightarrow{I_F} = 0$$

$$\overrightarrow{I_F} = \frac{\overrightarrow{V_S} - \overrightarrow{V_{PF}}}{jX_S}$$

Equation II.7 Current and voltage equation during the fault.

From the comparison between equation II.6 and equation II.7, we see that the fault current can be limited to the load current when $\overrightarrow{V_{PF}}$ is restored to $\overrightarrow{V_P}$. The SC injects a leading voltage $\overrightarrow{V_{SC}}$ until $\overrightarrow{V_{PF}}$ is restored into its prefault level $\overrightarrow{V_P}$ as shown in Figure II.8.

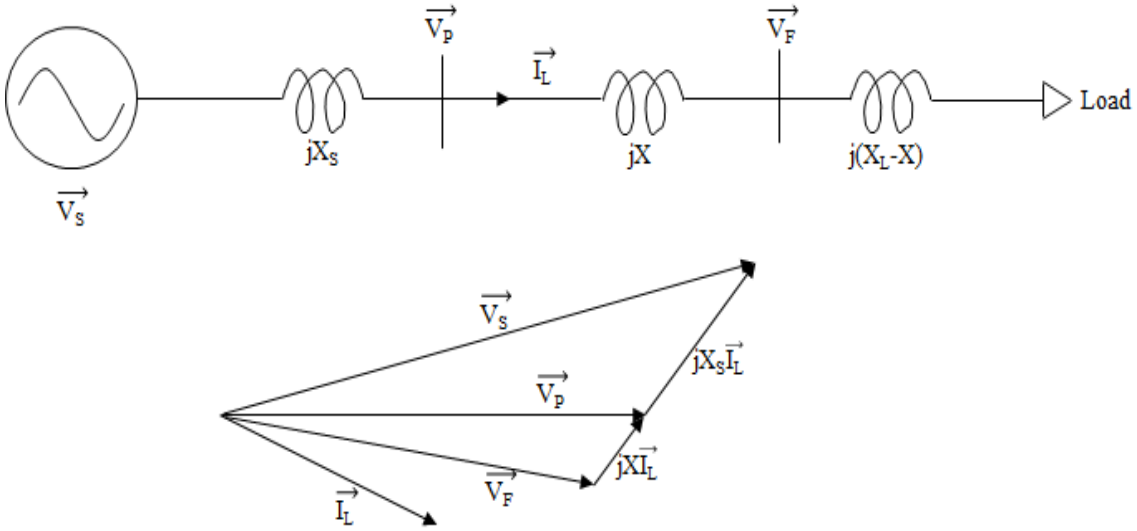

Figure II.7 Network model and phasor diagram under the prefault condition.

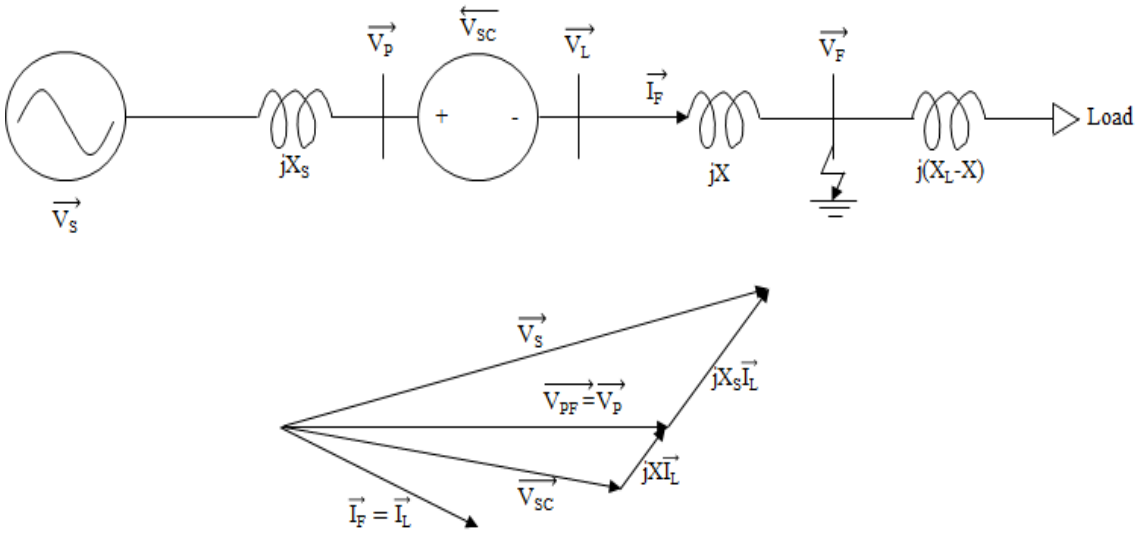

Figure II.8 Network model and phasor diagram under the load side fault condition.

Power Electronic Switches

A great deal of power electronics based FCLs have been proposed for fault current limitation and power system stability enhancement. With the development of power electronic devices and control technologies, a large number of Flexible AC Transmission Systems (FACTS) devices have been developed and are in operation extensively for the security enhancement of power systems [7]. FCLs using solid-state devices such as Insulated Gate Bipolar Transistor (IGBT), Silicon Controlled Rectifier (SCR), and Gate Turn-off Thyristor (GTO) can be classified into (1) Series Switch type FCL, (2) Bridge type FCL, and (3) Resonant FCL [8]. The basic operational principle of SSFCLs is almost same in that currents flow through zero impedance path in steady-state and they are switched into the fault current limiting reactor in case of short-circuit conditions. However, the configuration of SSFCLs can be different based on their application purpose. Different types of Series Switch type FCLs were described [9] and an application of a Thyristor-Controlled Series Reactor was presented to reduce furnace arc flicker [10]. Bridge-type FCLs using different types of switching device were also proposed [11, 12], and the influence of this type of FCL was investigated in terms of power system transient stability [13]. Another application using FACTS based Short-Circuit Current Limiter (SCCL) was suggested in [14], where thyristor Protected Series Compensator (TPSC) combined with an external reactor showed the benefits for fault current limitation and SSR mitigation. Transient stability was also evaluated with this type of series capacitor compensated FCL in [15]. Basic configurations for those FCLs are illustrated in Figure II.9.

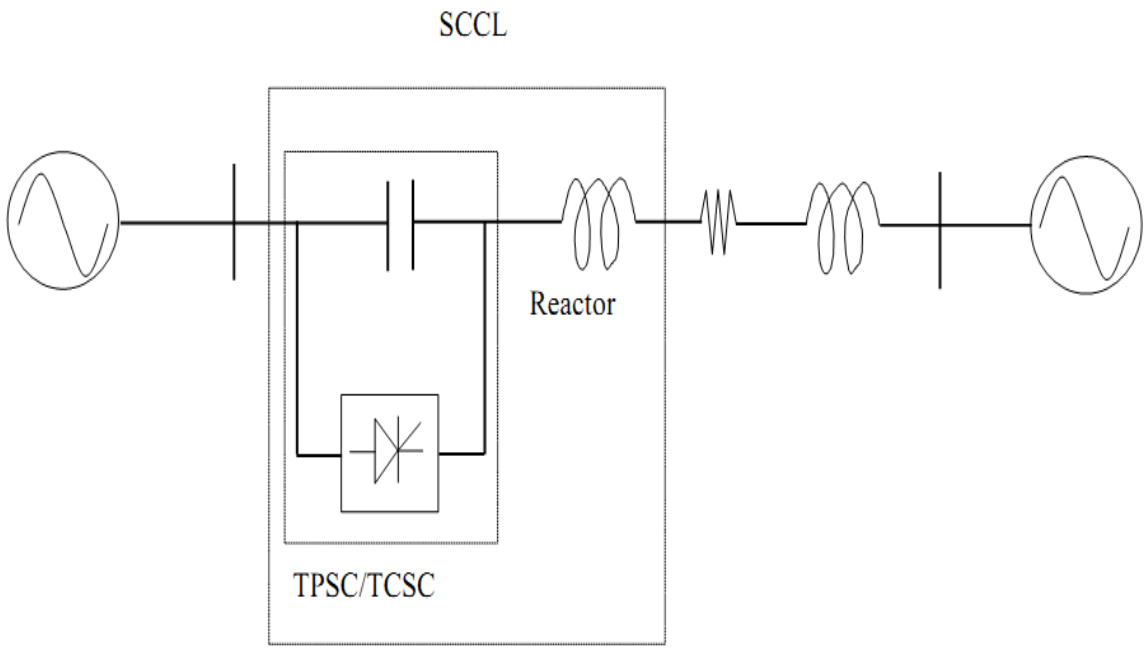

(a)

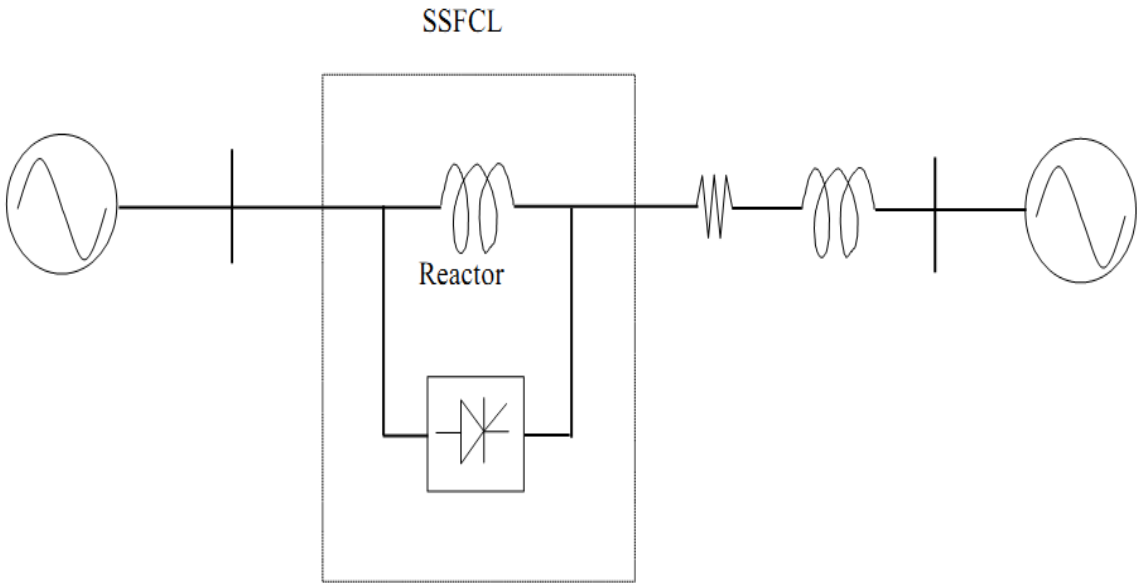

(b)

Figure II.9 FCL using power electronic switches (a) Short Circuit Current Limiter (SCCL), (b) Solid-State Fault Current Limiter (SSFCL).

CHAPTER III

POWER SYSTEM STABILITY

For the voltage and reactive power compensation, we usually use reactive power compensator such as static condensers, shunt reactors which are static reactive sources being used for steady state voltage regulations and thyristor controlled series condensers, thyristor controlled reactors which are dynamic reactive sources being used for transient stability enhancement.

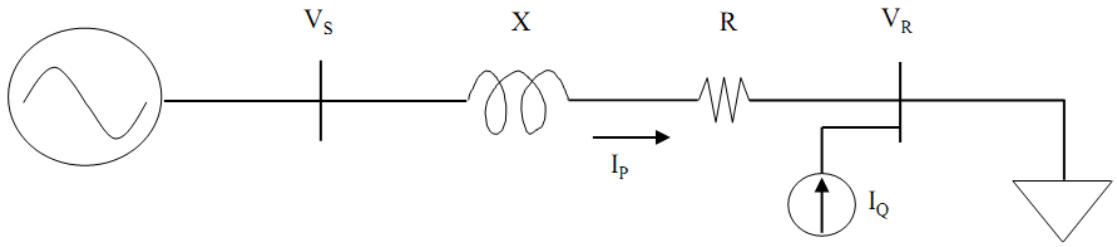

(a)

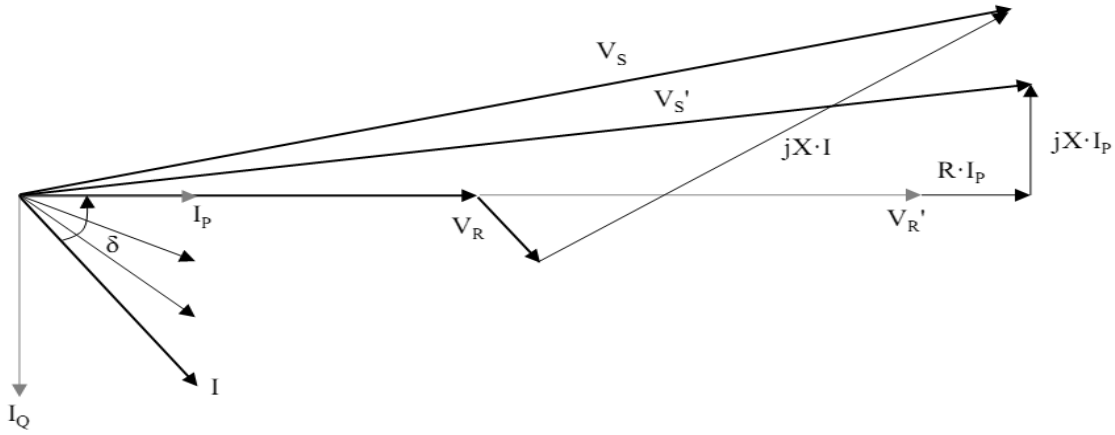

(b)

Figure III.1 Shunt compensation with a current source (a) Network configuration, (b) Phasor diagram: V_R can be controlled V_R to V'_R by compensating the reactive component of the load current.

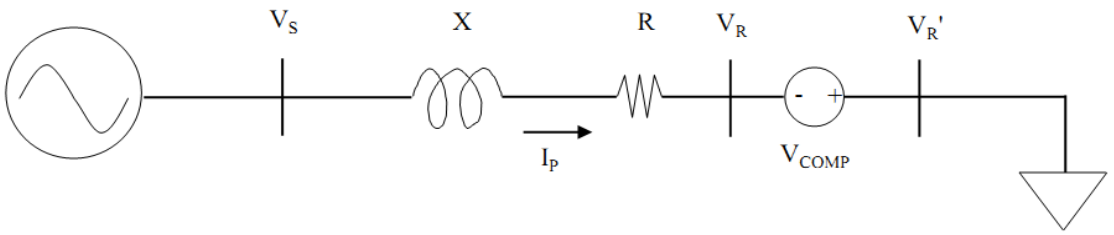

(a)

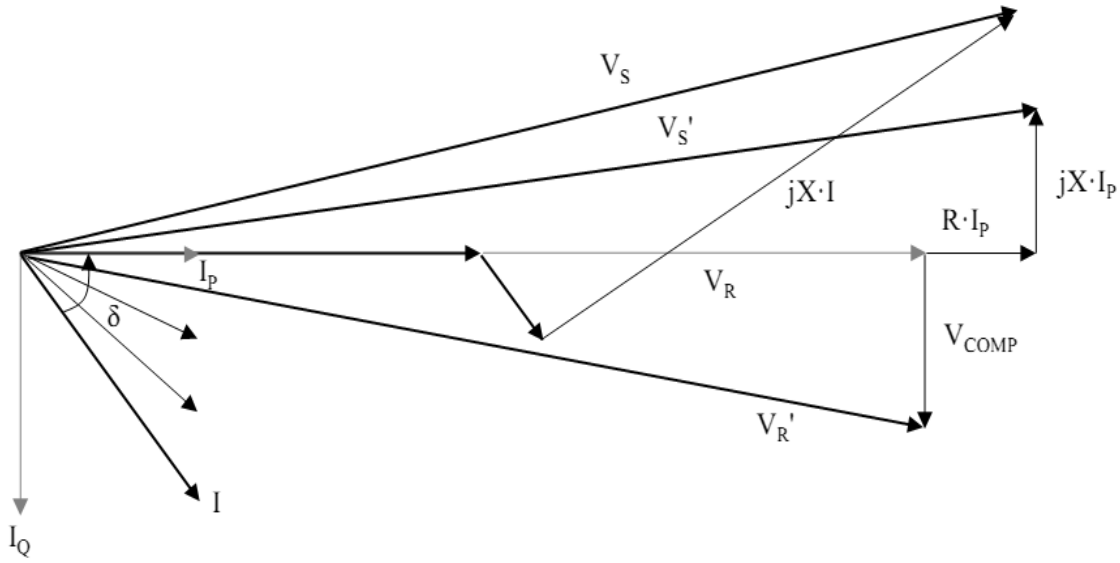

(b)

Figure III.2 Series compensation with a voltage source (a) Network configuration, (b) Phasor diagram: V_R can be controlled by inserting V_{COMP} and the appropriate magnitude control of V_{COMP}.

They can be connected to the system in series or in shunt. To reduce transmission losses and improve the voltage regulation and stability, we normally compensate reactive powers near the load. By injecting the reactive component of the current near the load, a compensator can control the current from the generator resulting in voltage regulation improvement in the load side. Considering leading compensation, we can increase the

load side voltage to V'_R with the same source voltage V_S. In addition, we can reduce relatively large amount of reactive losses compare to uncompensated system. Therefore, this kind of compensation is usually used for voltage stability enhancement. Figure III.1 shows the principle of shunt reactive power compensation in a simple AC circuit which can be represented as

$$V_S = V_R + I_P(R + jX)$$

Equation III.1 Voltage equation for simple AC circuit.

Based on the compensation types required, inductors or capacitors can be used. For independent control with the voltage at the connection point, current source or voltage source compensator can be used [16]. Var compensation can also be realized using series compensator. Typical series compensation is made by series capacitors and Figure III.2 shows the principles of series compensation in a radial AC system which can be represented as

$$V_S = V'_R + I_P(R + jX) - V_{COMP}$$

Equation III.2 Voltage equation for the series compensated AC system.

The voltage angle of V'_R can be changed by inserting V_{COMP} between the line and the load. With the appropriate magnitude control of V_{COMP}, V_R can be controlled. This kind of series compensation gives three main benefits to the transmission system. (1) Increase angular stability of the system (2) Improve voltage stability of the system (3) Optimize power sharing between parallel circuits. Equal Area Criterion is generally used to understand basic factors that influence the transient stability of power systems [17]. It basically uses the relationship between the rotor angle and the accelerating power.

$$\frac{d^2\delta}{dt^2} = \frac{w_0}{2H}(P_M - P_E)$$

Equation III.3 Relationship between the rotor angle and the accelerating power.

Where, P_M: mechanical power, P_E: electrical power, δ: rotor angle, in electrical radian, H: inertia constant, in MWs/MVA. Let us consider the response of single-machine infinite bus system to a three-phase fault on transmission line2, as shown in Figure III.3. Network conditions can be represented as: (1) Prefault (both circuits in service), (2) During a three-phase fault, (3) Postfault (circuit 2 out of service) and those are illustrated with P-δ plots in Figure III.4. Initially, the system is operating where $P_M = P_E$. When the fault occurs, P_E goes down to b. At this point, since P_M is greater than P_E, the rotor starts to accelerate until the fault is cleared. When the fault is cleared, the operating point shifts to d based on the line condition. However, since the rotor speed is greater than the synchronous speed, it continues to increase until the kinetic energy gained during the acceleration period is exhausted. The operating point moves to e, where the accelerating power is equal to the decelerating power. At point e, the rotor speed is equal to the synchronous speed, but P_E is greater than P_M. Therefore, the rotor starts to decrease the speed following the P-δ curve for the single circuit condition. In the presence of any source of damping, the rotor finally gets to a new stable operating point. With a delayed fault clearing, acceleration power is greater than deceleration power, leading to loss of synchronism.

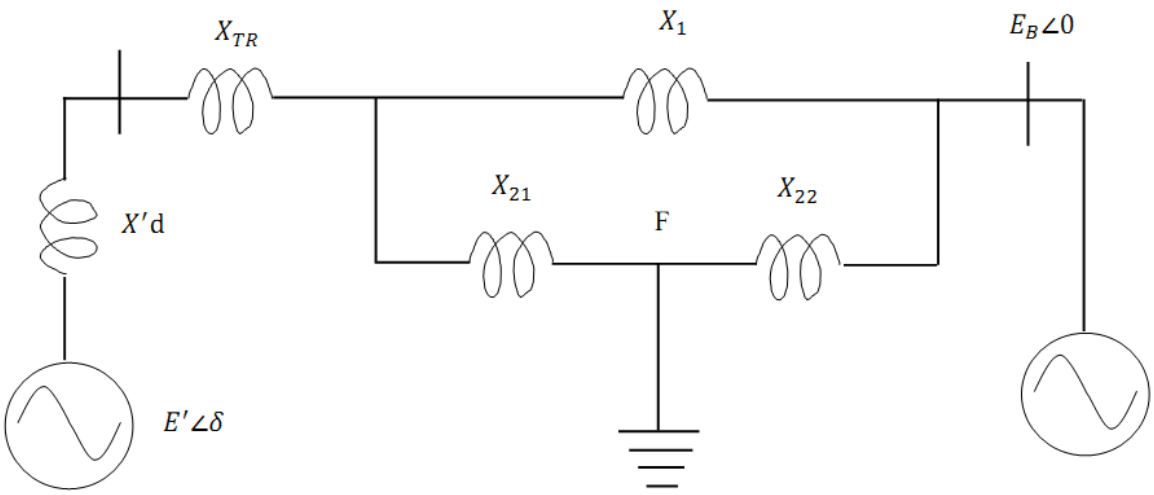

Figure III.3 Equivalent circuit of single-machine infinite bus system: a generator delivers power to an infinite bus through two transmission circuits.

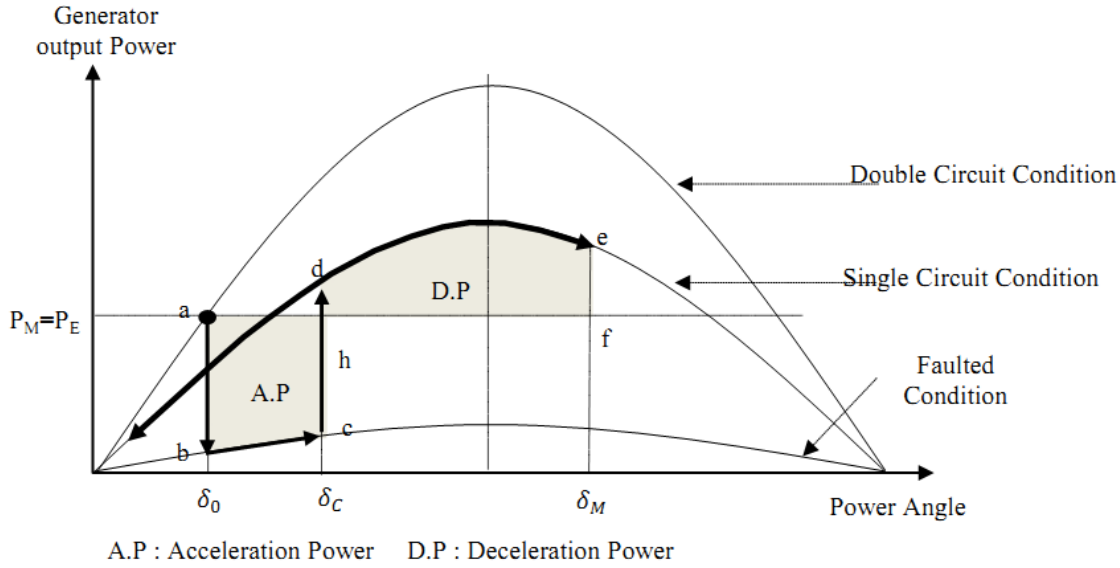

Figure III.4 Power-angel curve for Equal Area Criterion.

Thyristor Controlled Series Compensator (TCSC)

A typical TCSC consists of a Fixed Series Capacitor (FC) in parallel with a Thyristor Controlled Reactor (TCR). The bi-directional thyristor valves are red with a phase angle ranging between 90 and 180 with respect to the capacitor voltage. A Metal-

Oxide Varistor (MOV) is used to prevent the over-voltage across the capacitor. A circuit breaker is installed across the capacitor and it bypasses the capacitor when severe faults or equipment-malfunction events occur. Conduction losses of the TCSC valves can be minimized by installing an Ultra-High-Speed Contact (UHSC) across the valve. It is closed shortly after the thyristor valve is turned on, and opened shortly before the valve is turned off. During a sudden overload of the valve and fault conditions, the metallic contact is closed to alleviate the stress on the valve [18].

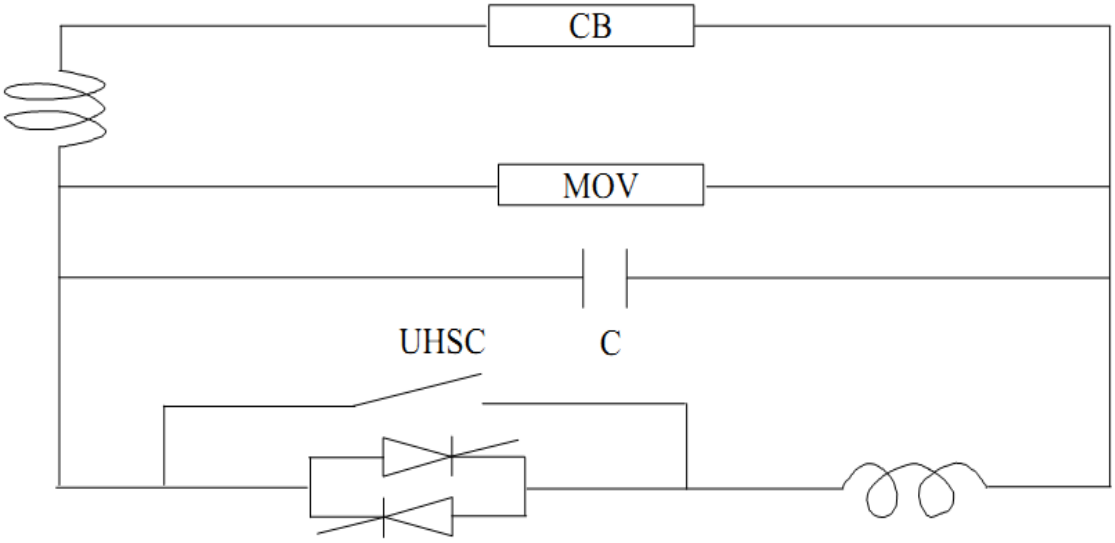

Figure III.5 A practical configuration of TCSC.

Figure III.5 shows a practical configuration of TCSC. The main capabilities of the TCSC can be achieved by changing the impedance of the line where it is connected, which can be done by controlling the firing angle of the thyristors. Variation of X_L with respect to firing angle and the equivalent impedance of the TCSC are given as the following equations

$$X_L(\alpha) = X_L \frac{\pi}{\pi - 2\alpha - 2\sin 2\alpha}, X_L \leq X_L(\alpha) \leq \infty$$

$$X_{TCSC}(\alpha) = X_C - \frac{{X_C}^2}{X_C - X_L} \times \frac{\sigma + \sin\sigma}{\pi} + \frac{4{X_C}^2}{X_C - X_L} \times \frac{\cos^2(\frac{\sigma}{2})}{k^2 - 1} \times \frac{k\tan\left(\frac{k\sigma}{2}\right) - \tan(\sigma^2)}{\pi}$$

Equation III.4 Equivalent impedance of TCSC.

Where, σ = 2(π-α) is the conduction angle of TCSC, and k = $\sqrt{\frac{X_C}{X_L}}$ is the compensation ratio. Figure III.4 shows the impedance characteristics of a TCSC.

The followings represent the main functions of a TCSC. (1) Damping of the power swings from local and inter-area oscillations, (2) Suppression of subsynchronous oscillations, (3) Voltage support, and (4) Reduction of the short-circuit current.

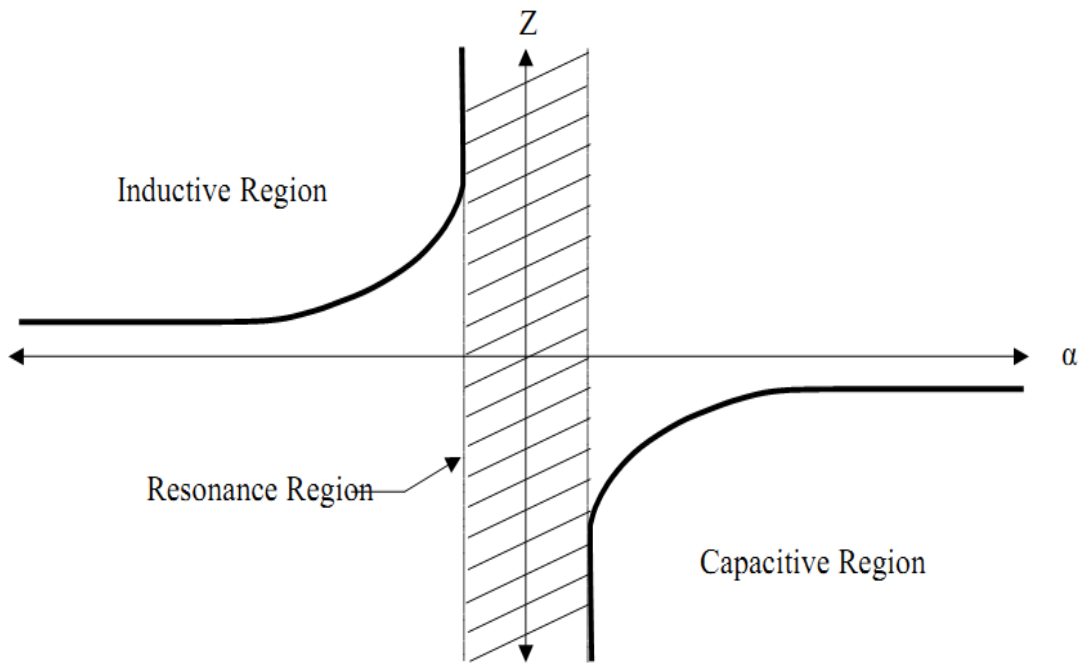

Figure III.6 Impedance characteristics of a TCSC with respect to firing angle.

Short Circuit Current Limiter (SCCL)

SCCL is developed from the series compensation which normally uses a capacitor to compensate the inductor used as a fault current limiter, thus the line is regarded as short-circuited. During normal operation, the FCL compensated with series capacitor increases the steady state stability limit. When a short-circuit fault occurs, the FCL can reduce the accelerating power at the initial stage of the fault and provide additional decelerating power at the fault clearing stage [15].

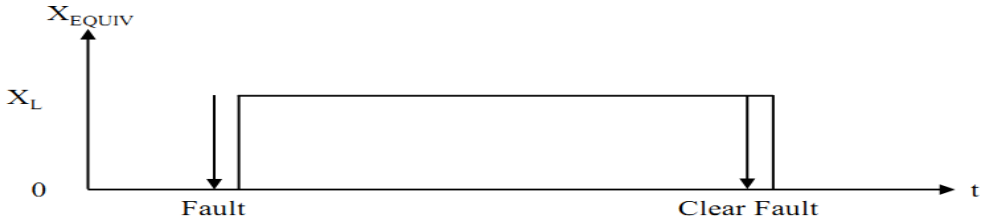

(a)

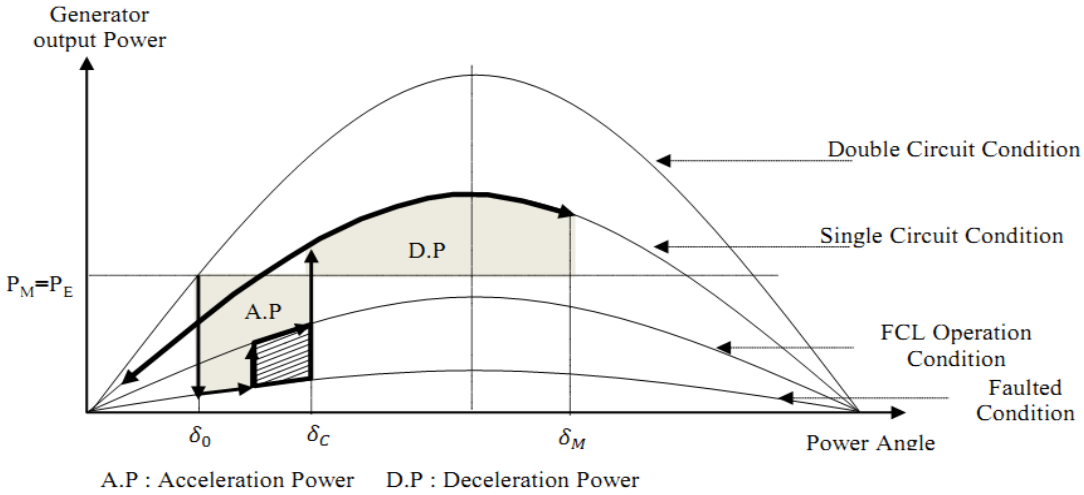

(b)

Figure III.7 The characteristics of SCCL and power-angle curve (a) During normal operation, equivalent impedance is treated as zero and XL during the fault (b) Accelerating power is decreased as much as the hatched area by inserting the series reactor.

Figure III.7 shows an example of a single line fault where double circuit transmission line becomes single circuit transmission line. The accelerating power will be decreased as much as the hatched area and power system synchronism can be maintained if the resultant accelerating power is smaller than the decelerating power.

CHAPTER IV

D-Q TRANSFORMATION

We transform time-varying voltage, current differential equations into time invariant differential equations. As it is not only easy to solve but also easy to understand and control. A, B, C phase variables in three phase AC system are transformed into orthogonal d, q, n axes variables [21]. Direct axis d represents the axis where excitation flux (or main flux) is and quadrature axis is 90 degree in electrical angle ahead to d axis in positive rotational direction and neutral axis is orthogonal to d-q axes in three dimensional spaces. Figure IV.1 represents axes of reference frames, where superscript s denotes stationary reference frame, e synchronous reference frame, w arbitrary rotating speed and Θ is defined as

$$\theta = \int_0^t w(\xi)d\xi + \theta(0) = \int_0^t w(\xi)d\xi$$

The transformation matrix can be derived as

$$f_{dqn}^{w} = T(\theta)f_{abc}$$

Equation IV.1 Transformation matrix.

The column vectors of variables are given as

$$f_{dqn}^{w} = [f_d^w \; f_q^w \; f_n^w]^T$$

$$f_{abc}^{w} = [\, f_a \; f_b \; f_c]^T$$

$$T(\theta) = \frac{2}{3}\begin{bmatrix} cos\theta & \cos\left(\theta - \frac{2}{3}\pi\right) & \cos\left(\theta + \frac{2}{3}\pi\right) \\ -sin\theta & -\sin\left(\theta - \frac{2}{3}\pi\right) & -\sin\left(\theta + \frac{2}{3}\pi\right) \\ \frac{1}{\sqrt{2}} & \frac{1}{\sqrt{2}} & \frac{1}{\sqrt{2}} \end{bmatrix}$$

Equation IV.2 Column vector and transformation matrix.

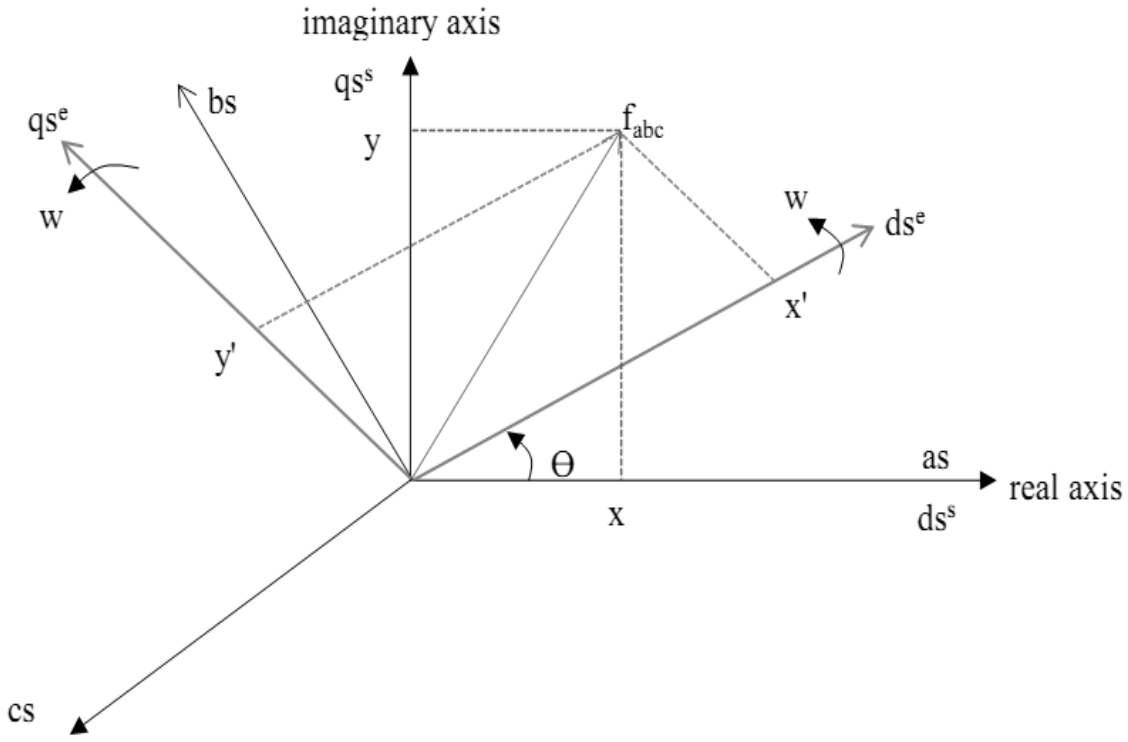

Figure IV.1 Axes of reference frame.

The variables in the three-phases axis can be converted both to the variables in the stationary reference frame and to the variables in the arbitrary reference frame as

$$f_{dqn}^{s} = T(0)f_{abc}$$

$$f_{dqn}^{w} = T(\theta)f_{abc} = R(\theta)T(0)f_{abc} = R(\theta)f_{dqn}^{s}$$

$$T(0) = \frac{2}{3}\begin{bmatrix} 1 & -\frac{1}{2} & -\frac{1}{2} \\ 0 & \frac{\sqrt{3}}{2} & -\frac{\sqrt{3}}{2} \\ \frac{1}{\sqrt{2}} & \frac{1}{\sqrt{2}} & \frac{1}{\sqrt{2}} \end{bmatrix}$$

$$R(\theta) = \begin{bmatrix} cos\theta & sin\theta & 0 \\ -sin\theta & cos\theta & 0 \\ 0 & 0 & 1 \end{bmatrix}$$

$$T(\theta) = R(\theta)\, T(0)$$

Equation IV.3 Conversion variables in different reference frames.

If the system is balanced, that is $f_a + f_b + f_c = 0$, and convert the variables in the three-phase axis to the variables in the stationary reference frame, then

$$f^s_{dqn} = T(0) f_{abc}$$

$$\begin{bmatrix} f^s_d \\ f^s_q \\ f^s_n \end{bmatrix} = \frac{2}{3}\begin{bmatrix} 1 & -\frac{1}{2} & -\frac{1}{2} \\ 0 & \frac{\sqrt{3}}{2} & -\frac{\sqrt{3}}{2} \\ \frac{1}{\sqrt{2}} & \frac{1}{\sqrt{2}} & \frac{1}{\sqrt{2}} \end{bmatrix}\begin{bmatrix} f_a \\ f_b \\ f_c \end{bmatrix}$$

$$f^s_d = \frac{2}{3}(f_a - \frac{1}{2} f_b - \frac{1}{2} f_c) = f_a$$

$$f^s_q = \frac{f_b - f_c}{\sqrt{3}}$$

$$f^s_n = 0$$

Equation IV.4 Conversion variables in the stationary reference frames.

Likewise, the variables in the synchronous reference frame can be converted with respect to the stationary reference frame as

$$f^e_{dqn} = R(\theta_e) f^s_{dqn}$$

$$\begin{bmatrix} f^e_d \\ f^e_q \\ f^e_n \end{bmatrix} = \begin{bmatrix} cos\theta_e & sin\theta_e & 0 \\ -sin\theta_e & cos\theta_e & 0 \\ 0 & 0 & 1 \end{bmatrix} \begin{bmatrix} f^s_d \\ f^s_q \\ f^s_n \end{bmatrix}$$

$$f^e_d = f^s_d \, cos\theta_e + f^s_q sin\theta_e$$

$$f^e_q = -f^s_d \, sin\theta_e + f^s_q cos\theta_e$$

Equation IV.5 Conversion variables in the synchronous reference frames.

As a result, when the space vector by three-phase components can be represented as the equation IV.7, three-phase variables can be represented by only two orthogonal components of a complex vector.

$$f_{abc} = \frac{2}{3}(f_a + a f_b + a^2 f_c)$$

$$f_n = \frac{1}{3}(f_a + f_b + f_c)$$

$$\mathrm{a} = e^{j\frac{2}{3}\pi} = cos\frac{2}{3}\pi + \mathrm{j}\sin\frac{2}{3}\pi = -\frac{1}{2} + j\frac{\sqrt{3}}{2}$$

Equation IV.6 Space vector represented by three-phase components.

The real part of f_{abc} equals to $\frac{2}{3}(f_a - \frac{1}{2}f_b - \frac{1}{2}f_c)$ which is correspondent to $f_s^{\,d}$ and the imaginary part of f_{abc} equals to $\frac{2}{3}(\frac{\sqrt{3}}{2}f_b - \frac{\sqrt{3}}{2}f_c)$ which is correspondent to $f_s^{\,q}$.

Consequently, the equation to transform a space vector fabc to the space vector in d-q axes which are stationary can be expressed as

$$f^s_{dq} = f^s_d + j f^s_q = f_{abc}$$

$$f^s_d = real(f_{abc})$$

$$f_q^s = imag(f_{abc})$$

Equation IV.7 Space vector in the stationary reference frame.

Likewise, from the previous relationship between the synchronous reference frame and stationary reference frame, and using Euler equation and basic vector modification, we can derive the transformation to other reference frame as

$$f_{dq}^e = f_d^e + jf_q^e = f_{dq}^s e^{-j\Theta_e} = f_{abc} e^{-j\Theta_e}$$

Equation IV.8 Transformation to other reference frame.

Inversely, we can extract the individual variables fa, fb, fc from the space vector f_{abc}.

$$real(f_{abc}) = \frac{2}{3}(f_a + af_b + a^2 f_c) = \frac{2}{3}f_a - \frac{1}{3}f_b - \frac{1}{3}f_c$$

$$real(a^2 f_{abc}) = \frac{2}{3}(a^2 f_a + f_b + af_c) = -\frac{1}{3}f_a + \frac{2}{3}f_b - \frac{1}{3}f_c$$

$$real(af_{abc}) = \frac{2}{3}(\mathrm{a}f_a + a^2 f_b + f_c) = -\frac{1}{3}f_a - \frac{1}{3}f_b + \frac{2}{3}f_c$$

$$f_n = \frac{1}{3}(f_a + f_b + f_c)$$

$$f_a = real(f_{abc}) + f_n$$

$$f_b = real(a^2 f_{abc}) + f_n$$

$$f_c = real(af_{abc}) + f_n$$

Equation IV.9 Individual variables f_a, f_b, f_c.

This approach is demonstrated with a specific R-L circuit shown in Figure V.1 (a) and parameters used in Table VI.1. Following figures are the voltage and current responses with respect to different duty ratios.

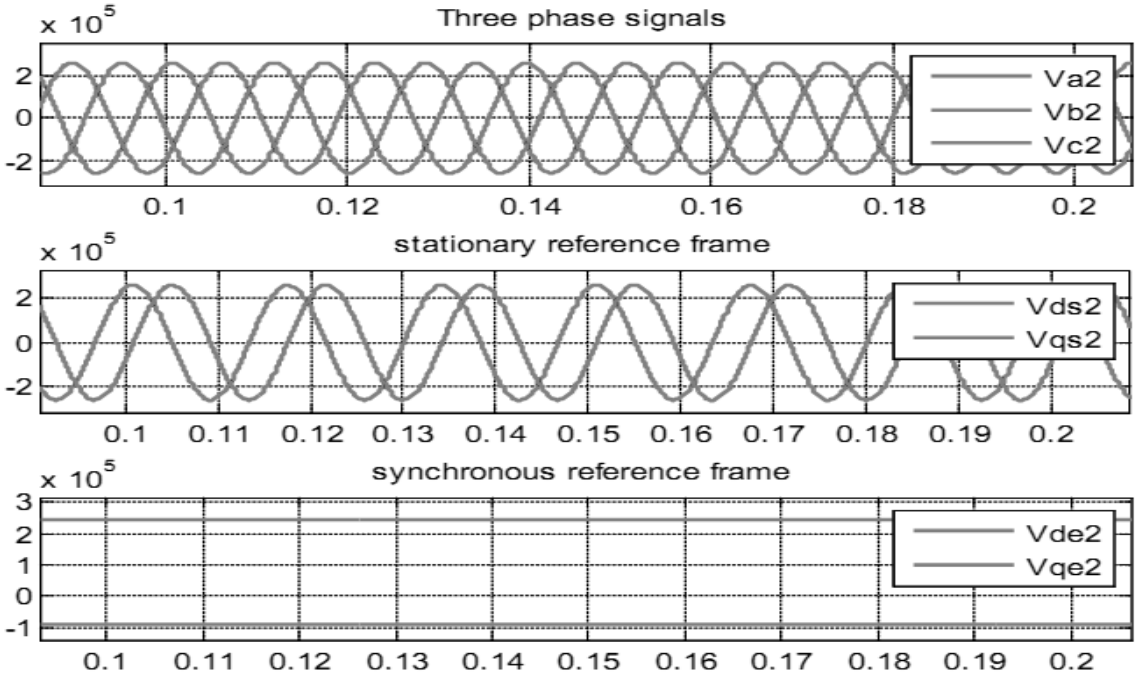

(a)

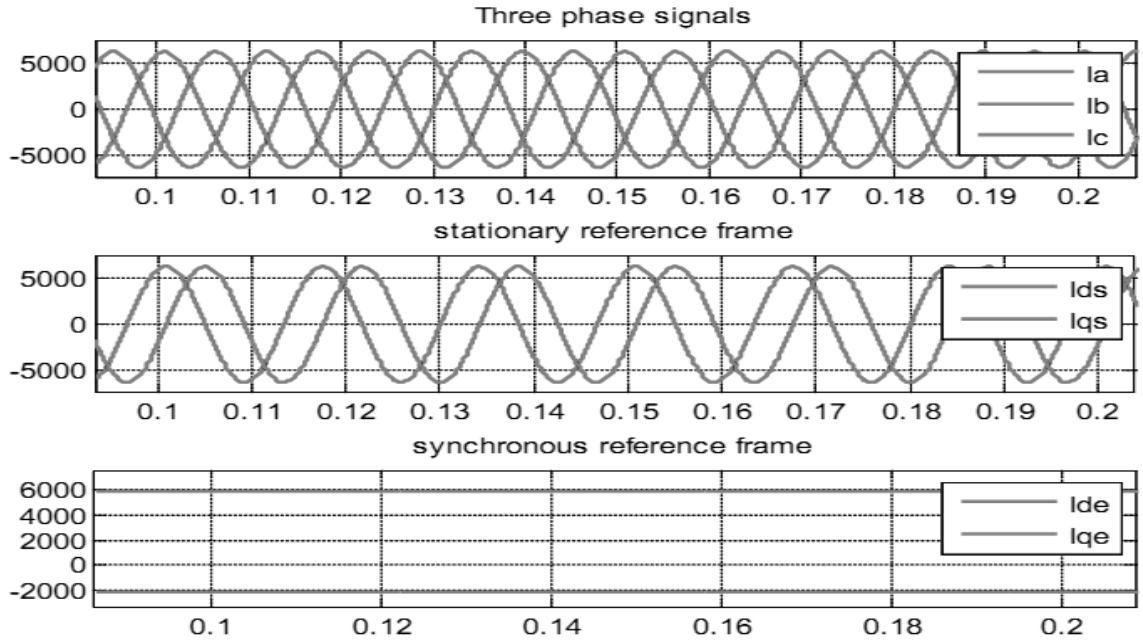

(b)

Figure IV.2 Voltage and current waveforms when duty ratio is 0 where the current flows only through the series reactor. (a) Load voltage (b) Current.

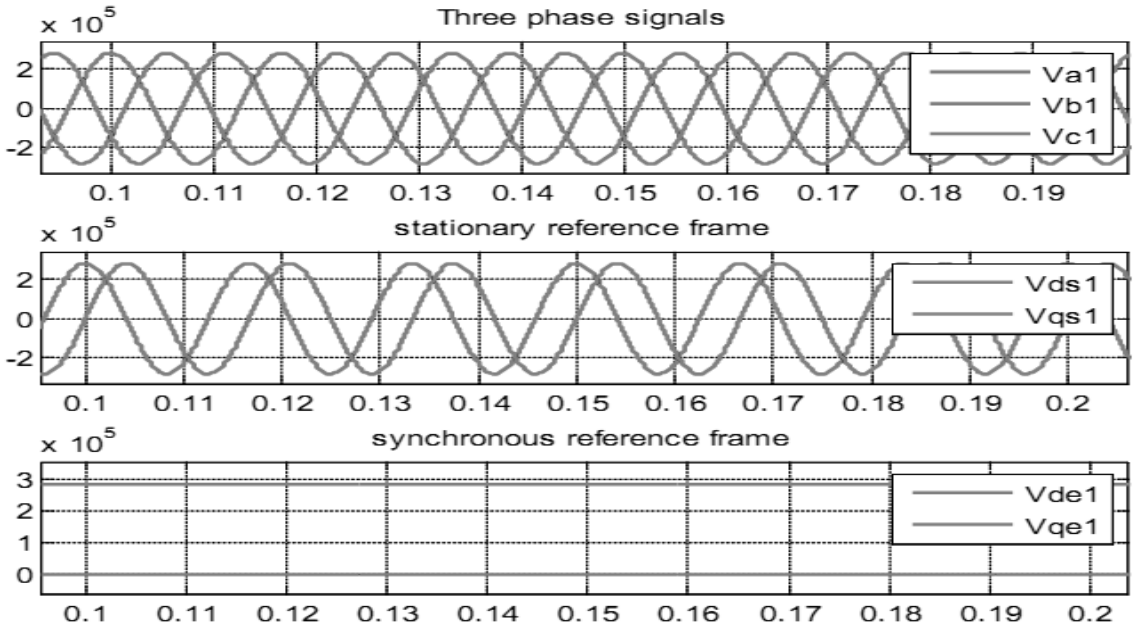

(a)

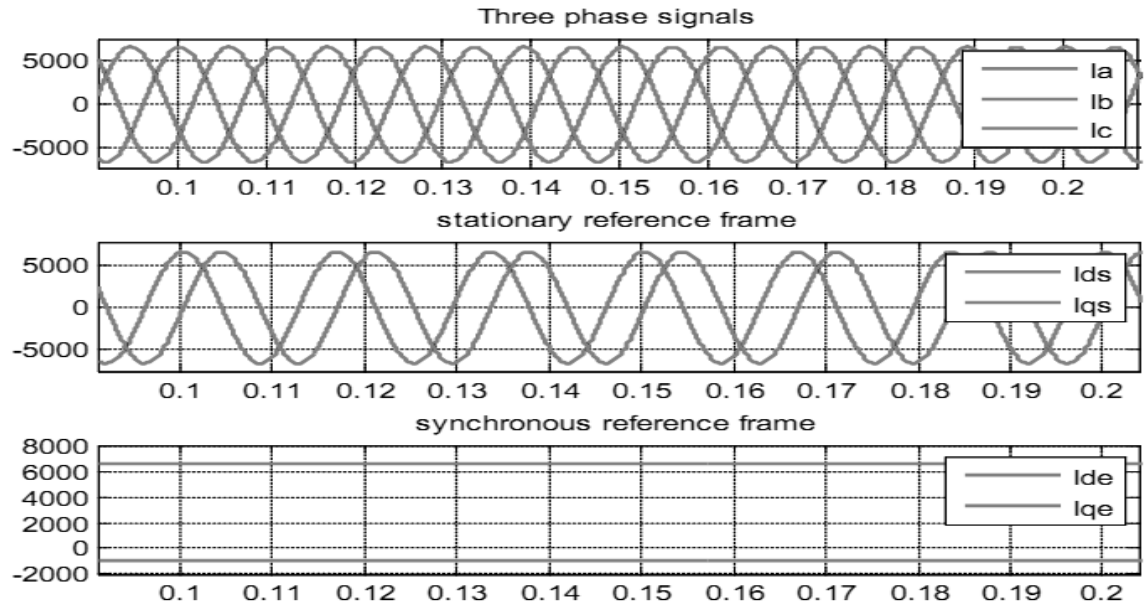

(b)

Figure IV.3 Voltage and current waveforms when duty ratio is 1 where the current flows only through the bypass switch. (a) Load voltage (b) Current.

CHAPTER V

PROPOSED APPROACH

In order to demonstrate the advantages of the TCSR, especially from the voltage point of view, a simple R-L circuit shown in Figure V.1 (a) is used. The receiving-end voltage is controlled by changing the equivalent impedance of FCL. To achieve this goal, following approach is proposed. A state-space model is constructed and averaged using d-q transformation method. Since the input (duty) and output (v_R) variables feature nonlinear relationships, linearization technique is applied to the averaged state-space model to obtain a system transfer function. A PI controller is designed to get a better dynamic response and zero steady-state error.

Voltage Stabilizing Fault Current Limiter

When the thyristor switch is open, the network in Figure V.1 (a) becomes as shown in Figure V.1 (b) and the voltage and current dynamic equations are given as

$$\overrightarrow{v_S} - L_T \frac{d\overrightarrow{\imath_L}}{dt} - R_T\overrightarrow{\imath_L} - L_{FCL}\frac{d\overrightarrow{\imath_L}}{dt} = R_L\overrightarrow{\imath_L}$$

$$\frac{d\overrightarrow{\imath_L^e}}{dt} = -\frac{R + jw(L_T + L_{FCL})}{(L_T + L_{FCL})}\overrightarrow{\imath_L^e} + \frac{\overrightarrow{v_s^e}}{(L_T + L_{FCL})}$$

$$\overrightarrow{v_R^e} = R_L\overrightarrow{\imath_L^e}$$

Equation V.1 Voltage and current equations in case the thyristor switches are open.

$\overrightarrow{x^e} = \vec{x}e^{-jwt}, R = R_L + R_T$, and the superscript e denotes synchronous reference frame. When the switch is closed, the network becomes like Figure V.1 (c) and the voltage and current dynamic equations become

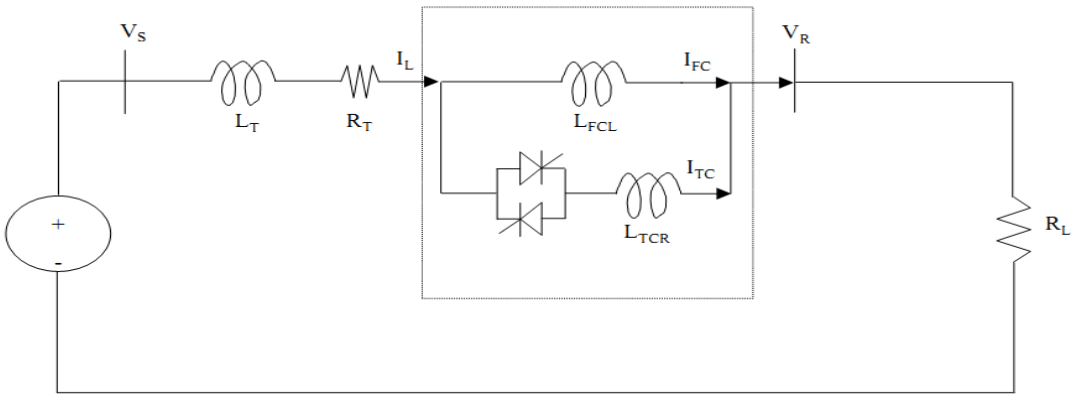

(a)

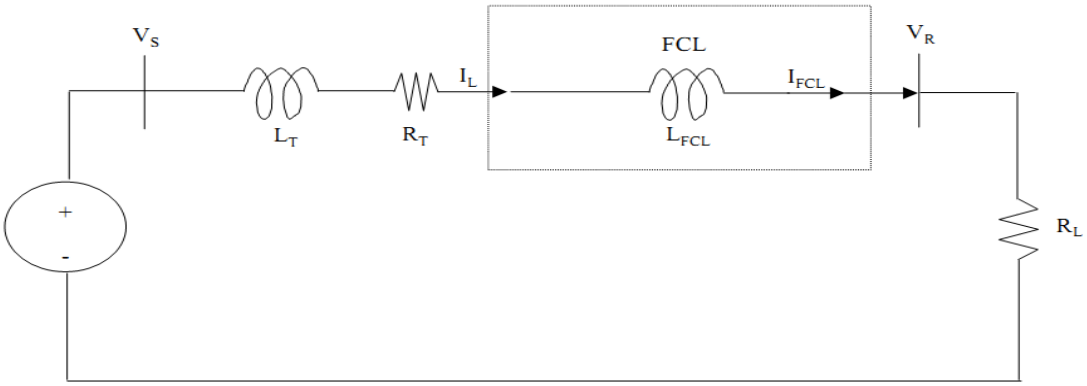

(b)

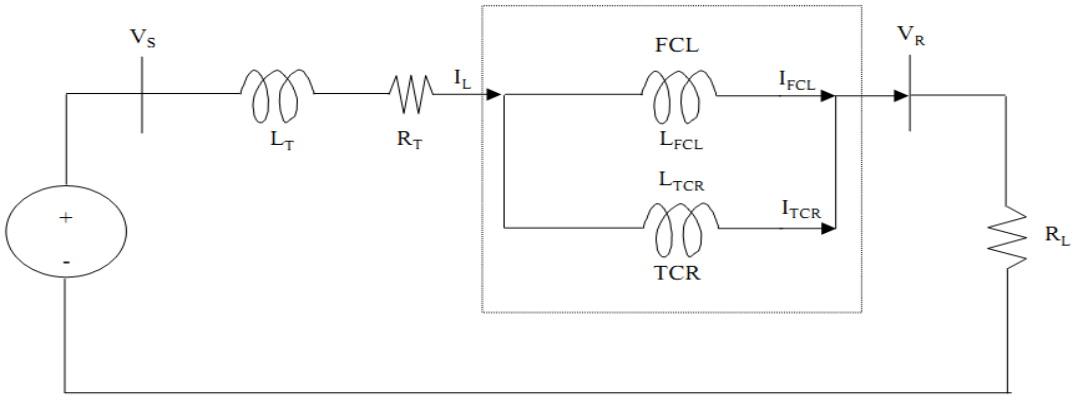

(c)

Figure V.1 Model for circuit analysis (a) Original circuit, (b) Equivalent circuit when switch is off, (c) Equivalent circuit when switch is on.

$$\overrightarrow{v_S} - L_T \frac{d\overrightarrow{i_L}}{dt} - R_T\overrightarrow{i_L} - L_{EQ} \frac{d\overrightarrow{i_L}}{dt} = R_L\overrightarrow{i_L}$$

$$\frac{d\overrightarrow{i_L^e}}{dt} = -\frac{R + jw(L_T + L_{EQ})}{(L_T + L_{EQ})}\overrightarrow{i_L^e} + \frac{\overrightarrow{v_s^e}}{(L_T + L_{EQ})}$$

$$\overrightarrow{v_R^e} = R_L\overrightarrow{i_L^e}$$

Equation V.2 Voltage and current equations in case the thyristor switches are close.

$L_{EQ} = L_{FCL}L_{TCR}/(L_{FCL}+L_{TCR})$. These equations can be arranged into a set of state equations as

$$\dot{x} = Ax + Bu$$

$$y = Cx + Du$$

Where, x: state variable, u: input variable, y: output variable.

As the average behavior of the system is dependent on the conduction time of the thyristors [19], if we define the conduction and off-conduction time as T_T and T_B respectively, we can rewrite the previous equations into two sets of state equations depending on the different conduction stages

$$\dot{x_T} = (A_T x + B_T u)T_T$$

$$\dot{x_B} = (A_B x + B_B u)T_B$$

Where $T_S = T_T + T_B$: switching time, and subscript T and B denote ON and OFF, respectively. The averaged model for the system can be expressed as the following set of state equations

$$\dot{x} = (A_T d_T + A_B d_B)x + (B_T d_T + B_B d_B)u$$

$$= A_T x + B_T u + d(A_B - A_T)x + d(B_B - B_T)u$$

$$y = C_T(1 - d)x + dC_B x$$

$$d_T = T_T/T_S = 1\text{-}d,\ d_B = T_B/T_S = d$$

Applying this relationship into the system model equations V.1, V.2, then,

$$\frac{d\vec{i_L^e}}{dt} = -\frac{R + jw(L_T + L_{FCL})}{(L_T + L_{FCL})}\vec{i_L^e} + \frac{\vec{v_s^e}}{(L_T + L_{FCL})} + d\{\frac{R + jw(L_T + L_{FCL})}{(L_T + L_{FCL})} - \frac{R + jw(L_T + L_{EQ})}{(L_T + L_{EQ})}\}\vec{i_L^e} + d\{\frac{1}{(L_T + L_{EQ})} - \frac{1}{(L_T + L_{FCL})}\}\vec{v_s^e}$$

$$\vec{v_R^e} = R_L\vec{i_L^e}$$

Equation V.3 Averaged voltage and current dynamic equations.

As a result, the voltage drop on the fault current limiting reactor can be limited by the following factor and controlled by duty d.

$$d\{\frac{R + jw(L_T + L_{FCL})}{(L_T + L_{FCL})} - \frac{R + jw(L_T + L_{EQ})}{(L_T + L_{EQ})}\}\vec{i_L^e} + d\{\frac{1}{(L_T + L_{EQ})} - \frac{1}{(L_T + L_{FCL})}\}\vec{v_s^e}$$

Plant Model and Compensator Design

However, the system model is nonlinear because the duty is also a function of time. Therefore, we need to linearize the non-linear equation to solve. Considering non-linear function $F(Z)$ and applying Taylor formula at $Z = Z_0$, the linearized function can be approximated as

$$F(Z) \approx F(Z_0) + \frac{\partial F}{\partial Z}(Z - Z_0)$$

Equation V.4 Linearized function.

For the controller design, we define state variable, input, and output vector as

$$x = [\vec{i_L}],\qquad u = \begin{bmatrix}\vec{v_S} \\ d\end{bmatrix},\qquad y = [\vec{v_R}]$$

, then the state equations can be written as

$$\dot{x} = F(\vec{\imath_L}, \vec{v_S}, d)$$

$$y = G(\vec{\imath_L}, \vec{v_S}, d)$$

If we apply linearization method at an operating point where steady state values are I_L, V_S, D, V_R, X, U, the dynamic model can be expressed with steady-state terms and linear small signal terms as

$$\frac{d}{dt}\vec{\imath_L} = F(X,U) + \frac{\partial F}{\partial i_L}(\vec{\imath_L} - I_L) + \frac{\partial F}{\partial v_S}(\vec{v_S} - V_S) + \frac{\partial F}{\partial d}(d - D)$$

$$\vec{v_R} = G(X,U) + \frac{\partial G}{\partial i_L}(\vec{\imath_L} - I_L) + \frac{\partial G}{\partial v_S}(\vec{v_S} - V_S) + \frac{\partial G}{\partial d}(d - D)$$

Equation V.5 Dynamic model including steady-state term and linear small signal term.

From these equations, we get the following linearized small signal dynamic model of the system.

$$\frac{d}{dt}\vec{\tilde{\imath}_L} = \frac{\partial F}{\partial i_L}\vec{\tilde{\imath}_L} + \frac{\partial F}{\partial v_S}\vec{\tilde{v}_S} + \frac{\partial F}{\partial d}\tilde{d}$$

$$\vec{\tilde{v}_R} = \frac{\partial G}{\partial i_L}\vec{\tilde{\imath}_L} + \frac{\partial G}{\partial v_S}\vec{\tilde{v}_S} + \frac{\partial G}{\partial d}\tilde{d}$$

$$\vec{\imath_L} = \vec{\tilde{\imath}_L} + \vec{I_L}, \vec{v_S} = \vec{\tilde{v}_S} + \vec{V_S}, \mathrm{d} = \tilde{d} + D$$

Equation V.6 Linearized small signal dynamic model.

Rewriting the equations leads to the following form as

$$\vec{\dot{\tilde{\imath}}_L} = \tilde{A}\vec{\tilde{\imath}_L} + \widetilde{B_{vs}}\vec{\tilde{v}_S} + \widetilde{B_d}\tilde{d}$$

$$\vec{\tilde{v}_R} = \tilde{C}\vec{\tilde{\imath}_L} + \widetilde{D_{vs}}\vec{\tilde{v}_S} + \widetilde{D_d}\tilde{d}$$

, and applying superposition rule gives the following control transfer functions ($\widetilde{v_S}$ = 0).

$$\frac{\widetilde{\vec{\imath_L}}}{\tilde{d}} = (sI - \tilde{A})^{-1}\widetilde{B_d}$$

$$\frac{\widetilde{\vec{v_R}}}{\tilde{d}} = \tilde{C}(sI - \tilde{A})^{-1}\widetilde{B_d}$$

$$\tilde{A} = \begin{bmatrix} \frac{R(D-1)}{(L_T + L_{FCL})} - \frac{RD}{(L_T + L_{EQ})} & w \\ -w & \frac{R(D-1)}{(L_T + L_{FCL})} - \frac{RD}{(L_T + L_{EQ})} \end{bmatrix}$$

$$\widetilde{B_d} = \begin{bmatrix} \left\{\frac{R}{(L_T + L_{FCL})} - \frac{R}{(L_T + L_{EQ})}\right\} I_{LD} \\ \left\{\frac{R}{(L_T + L_{FCL})} - \frac{R}{(L_T + L_{EQ})}\right\} I_{LQ} \end{bmatrix}$$

$$\tilde{C} = \begin{bmatrix} R_L & w \\ -w & R_L \end{bmatrix}$$

Equation V.7 Control transfer functions.

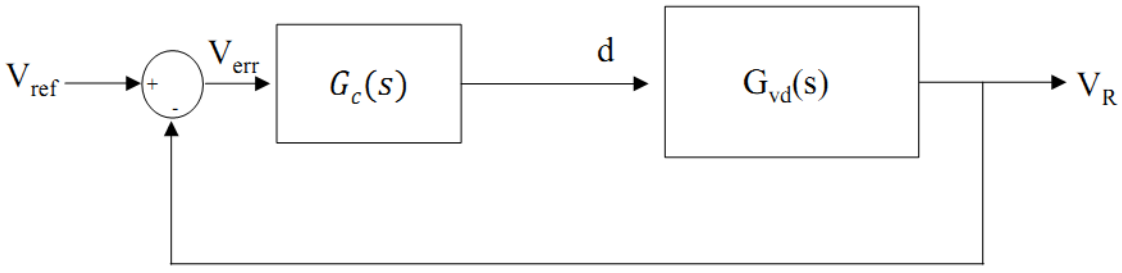

Figure V.2 PI regulator with negative feedback.

In the synchronous d-q reference frame, AC quantities can be treated as DC. In addition, by aligning the voltage vector to the d-axis, the output voltage of the q-axis can be set to zero. Therefore, substituting the equation V.7 with the derived values $\tilde{A}, \widetilde{B_d}, \tilde{C}$, we obtain the following transfer function.

$$G_{vd}(s) = \frac{\overrightarrow{\tilde{v}_{Rd}}}{\tilde{d}} = \frac{K_2 R_L I_{LD} s - K_1 K_2 R_L I_{LD} + K_2 R_L I_{LQ} w}{s^2 - 2K_1 s + {K_1}^2 + w^2}$$

$$K_1 = -\frac{R}{L_T + L_{FCL}} + RD\left(\frac{1}{L_T + L_{FCL}} - \frac{1}{L_T + L_{EQ}}\right)$$

$$K_2 = R\left(\frac{1}{L_T + L_{FCL}} - \frac{1}{L_T + L_{EQ}}\right)$$

Equation V.8 Control transfer function for the plant model.

Our plant and compensator transfer function can be expressed with $G_{vd}(s)$ and $G_c(s)$ in Figure V.2. To improve low-frequency loop gain and regulation, a PI compensator is designed.

$$G_c(s) = K_P + \frac{K_I}{s}$$

Equation V.9 A PI compensator model.

The closed-loop transfer function is given as

$$\frac{V_R}{V_{ref}} = \frac{\mathrm{T}}{1 + T}$$

Equation V.10 Closed-loop transfer function.

The loop gain $T = G_c(s) \cdot G_{vd}(s)$.

Routh's Stability Criterion can be used to determine the ranges of coefficients of polynomials for stability [20]. Considering the characteristic equation of an nth order system, the Routh array can be arranged as the following form

$$H(s) = s^n + a_1 s^{n-1} + a_2 s^{n-2} + \cdots + a_{n-1} s + a_n$$

Row	n	s^n	:	1	a_2	$a_4 \cdots$
Row	n-1	s^{n-1}	:	a_1	a_3	$a_5 \cdots$
Row	n-2	s^{n-2}	:	b_1	b_2	$b_3 \cdots$
Row	n-3	s^{n-3}	:	c_1	c_2	$c_3 \cdots$
:	:	:		:	:	:
Row	2	s^2	:	*	*	
Row	1	s^1	:	*		
Row	0	s^0	:	*		

$$b_1 = \frac{a_1 a_2 - a_3}{a_1}, b_2 = \frac{a_1 a_4 - a_5}{a_1}$$

$$c_1 = \frac{b_1 a_3 - a_1 b_2}{b_1}, c_2 = \frac{b_1 a_5 - a_1 b_3}{b_1}$$

A necessary and sufficient condition for stability is that all the elements in the first column of the Routh array are positive and it is shown that it is true for equation V.8 and V.9.

CHAPTER VI

COMPUTER SIMULATIONS

Duty Control to Increase Output Voltage

This approach is demonstrated with the R-L circuit shown in Figure V.1 and parameters used for the simulation are shown in Table VI.1. The transfer function of the plant model can be derived from V.8, which is given as

$$G_{vd}(s) = \frac{\overrightarrow{\widetilde{v_{Rd}}}}{\tilde{d}} = \frac{1204s + 1.261 \times 10^6}{s^2 + 2094s + 1.096 \times 10^6}$$

It has a constant steady state error, because the plant model has a small value when s = 0. To eliminate the steady state error, we have designed PI compensator, which gives the open-loop transfer function as

$$\mathrm{T} = (K_P + \frac{K_I}{s}) \frac{1204s + 1.261 \times 10^6}{s^2 + 2094s + 1.096 \times 10^6}$$

The characteristic equation of the close-loop transfer function as

$$1 + \mathrm{T} = s^3 + (2094 + 1204K_P)s^2 + (1.261 \times 10^6 K_P + 1204K_I + 1.096 \times 10^6)s + 1.261 \times 10^6 K_I$$

Applying Routh's Stability Criterion to the characteristic equation of the close-loop transfer function gives $K_P = 0.8$ and $K_I = 100$. As a result, the PI compensated transfer function becomes

$$\mathrm{T} = \mathrm{G}_c(s)G_{vd}(s) = \frac{963.5s^2 + 1.129 \times 10^6 s + 1.261 \times 10^8}{s^3 + 2094s^2 + 1.096 \times 10^6 s}$$

Steady state error is eliminated and the bus voltage can be enhanced by controlling the duty ratio of the TCSR. The output voltages are controlled from 245kV to 270kV based

on the duty ratio which starts to increase from 0.5sec. The step responses of the system and the output voltage responses with respect to different duty ratios are shown in Figures VI.1 and VI.2. Simulations are done with MATLAB.

Table VI.1 Simulation parameters

V_S	R_T	R_L	L_T	L_{FCL}	L_{TCR}
345kV	0.82Ω	41.06Ω	0.015H	0.025H	0.00025H

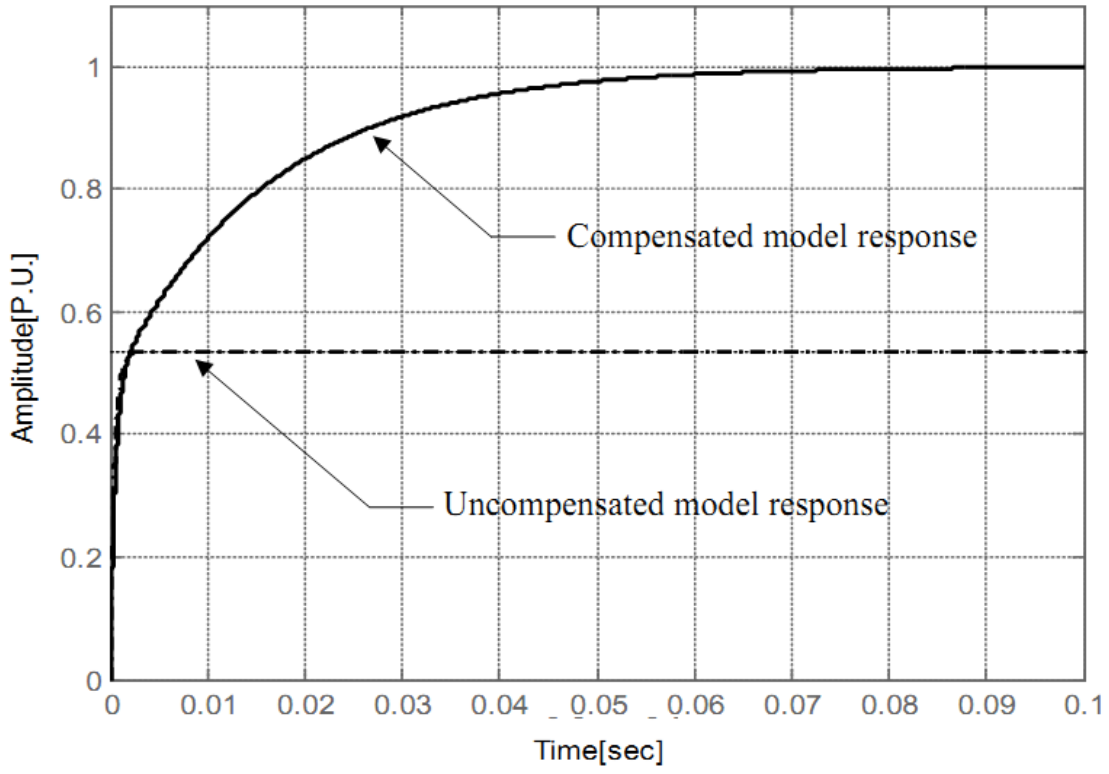

Figure VI.1 Step responses of the plant: Uncompensated model has a steady state error (0.4651), which is eliminated by a PI controller where K_P=0.8, K_I=100.

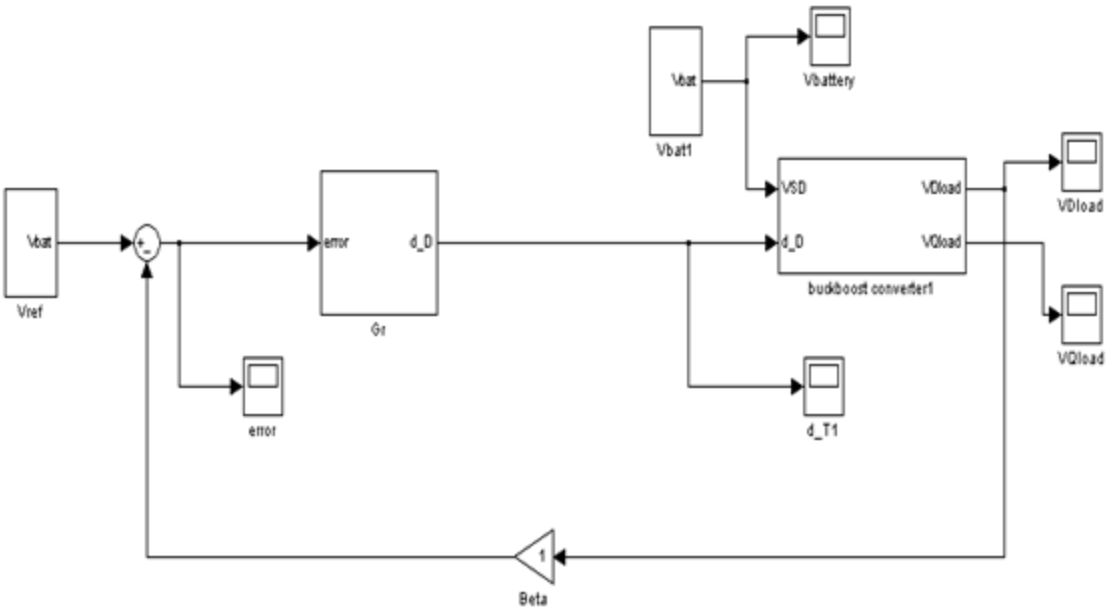

(a)

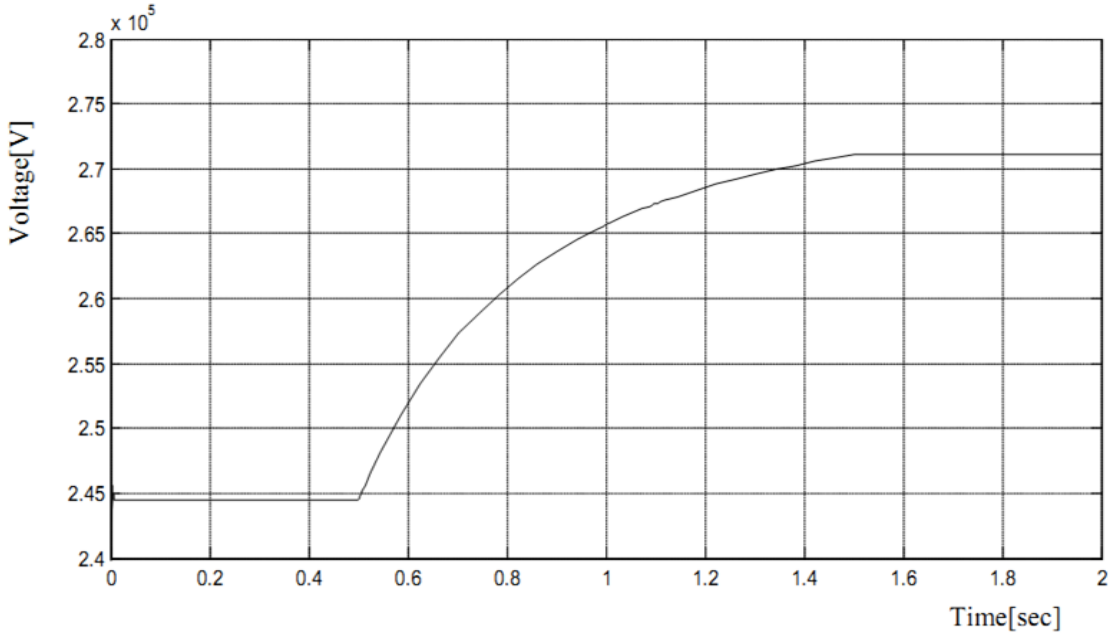

(b)

Figure VI.2 Overall model configuration and the output voltage responses: the output voltage changes from about 245kV to 270kV based on the duty ratio which starts to increase from 0.5sec.

Effects of TCSR on Different Fault Locations

Because the network is more complex than the simple R-L circuit in Figure V.1 (a), we need to consider faults that occur at different locations, e.g., near or far from the TCSR. When the fault occurs near the TCSR, the fault current will be high and the voltage will be low. Then the TCSR is required to operate as a fault current limiter and voltage restorer. On the other hand, when the fault occurs at a location far away from the TCSR, both the fault current and the voltage will be low. Then it does not need to act as a fault current limiter, but as a voltage restorer. This has been shown by PSCAD/EMTDC model shown in Figure VI.3.

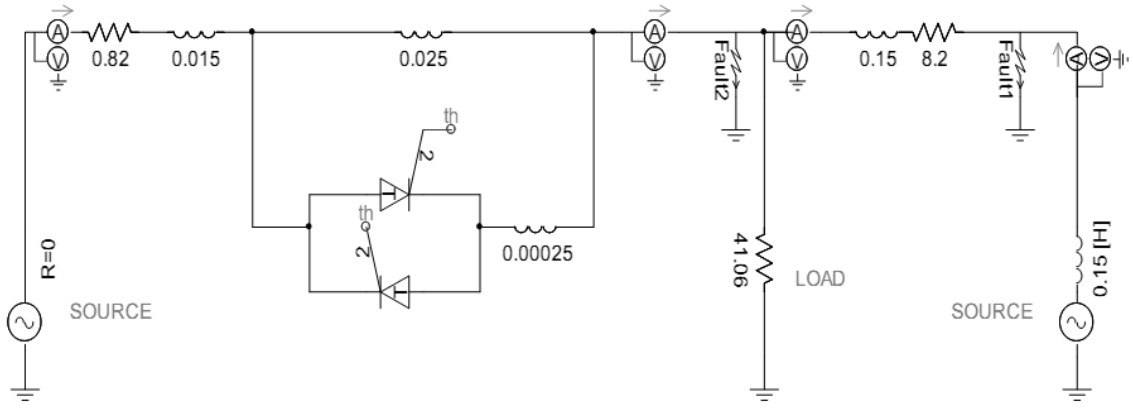

Figure VI.3 Typical power system model to investigate the effects of TCSR on fault currents and voltage dips: faults can be occurred either near the TCSR or far away from it.

The fault current is confined within nominal short-circuit current level with the series reactors and voltage drop due to the series reactor is around 4% which can be derived from the following equation [1].

$$\left|\frac{\Delta V}{V_N}\right| = 1 - \frac{1}{\sqrt{1 + 2V_k\sqrt{1-\cos^2\emptyset} + {V_k}^2}}$$

, where, $\frac{\Delta V}{V_N}$: system voltage drop, V_k: reactor short-circuit voltage, and cosΦ: power factor. In this system, possible issues are fault current problems in case the faults occur near the TCSR and under-voltage problems when the faults occur far away from the TCSR. Control actions of the TCSR enhance the voltages and limit the fault currents within nominal ranges. It can be seen that the fault currents for the near fault are limited within 40kA, which is the nominal short-circuit current, and the voltages are maintained higher in both cases. Figures VI.4, VI.5 and Table VI.2 show the simulation results.

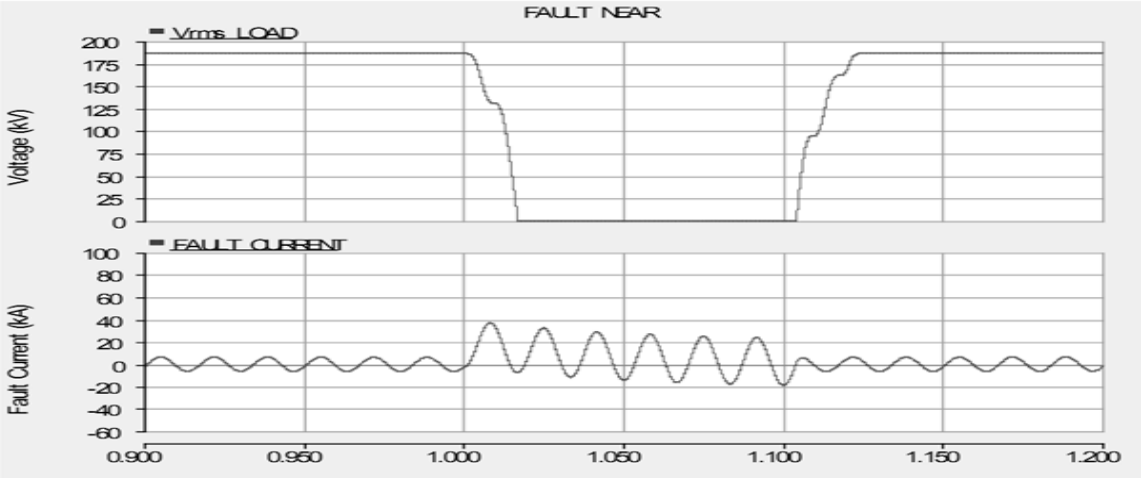

(a)

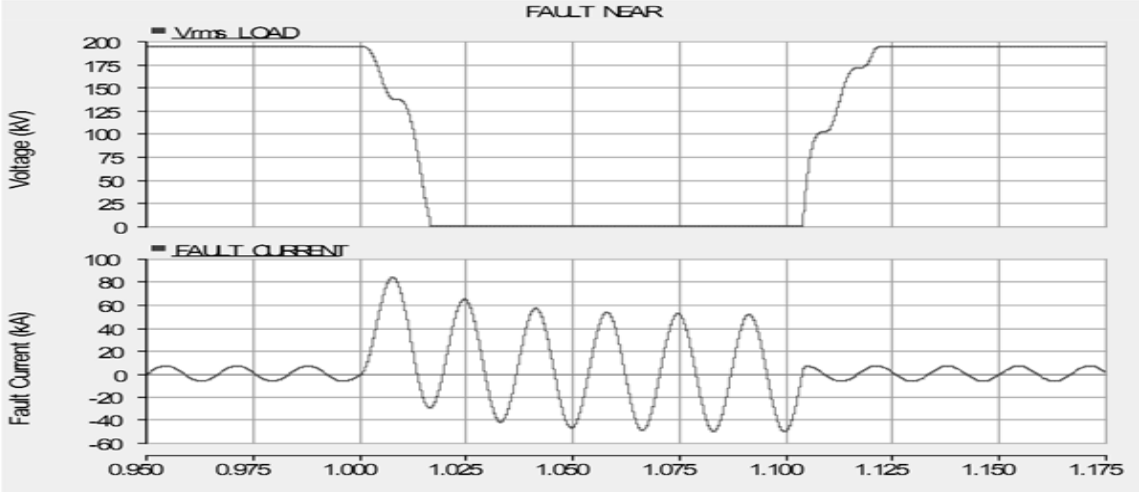

(b)

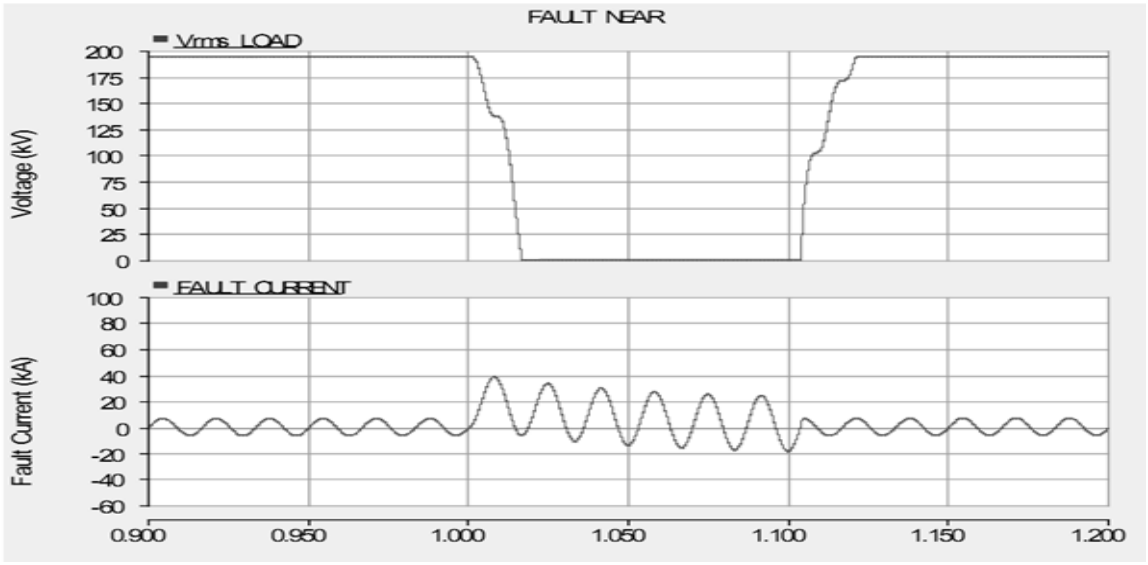

(c)

Figure VI.4 Simulation results for the fault near the TCSR: The TCSR is required to be operated as fault current limiter and voltage restorer. (a) The bus voltage is operating in low level when the series reactor is inserted. (b) The fault current is exceeding the nominal value when the series reactor is bypassed. (c) Voltage is maintained higher and the fault current is limited within nominal value when the control scheme is applied.

(a)

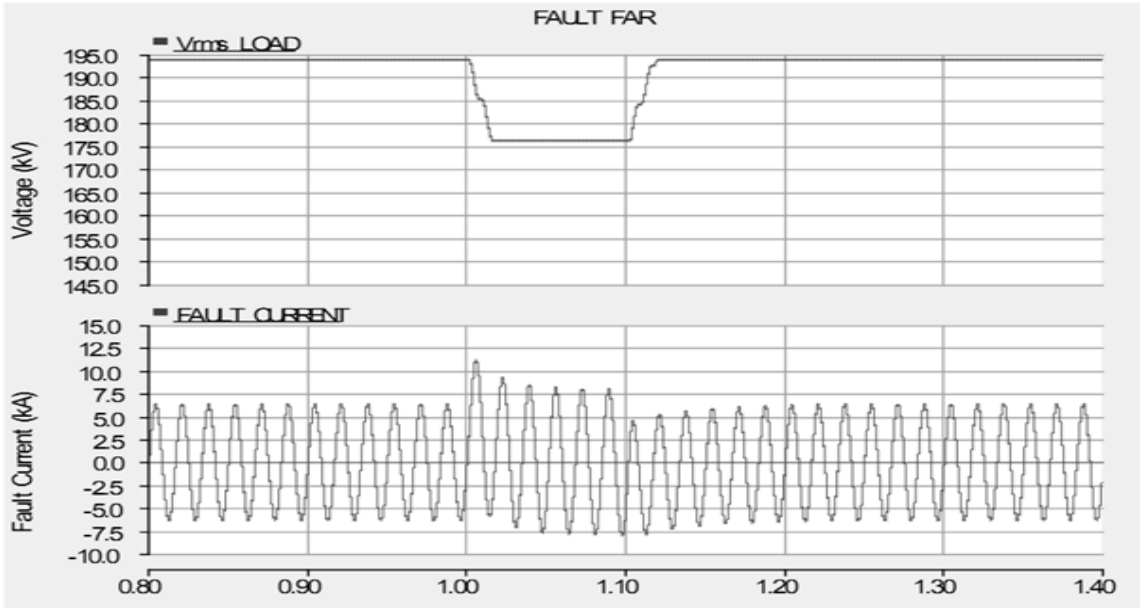

(b)

(c)

Figure VI.5 Simulation results for the fault far away from the TCSR: The TCSR is required to be operated as voltage restorer. (a) The bus voltage is operating in low level when the series reactor is inserted. (b) The voltage is maintained higher and the fault current is in low level when the series reactor is bypassed. (c) Voltage is maintained higher and no control action is required to limit the fault current.

Effects of TCSR on Bulk Power System Voltage Stability

To assess the benefits of the TCSR from the stability point of view, computer simulations have been performed with a bulk power system where the total demand is 73,000MW. A typical power system shown in Figure VI.6 is used for the voltage stability assessment.

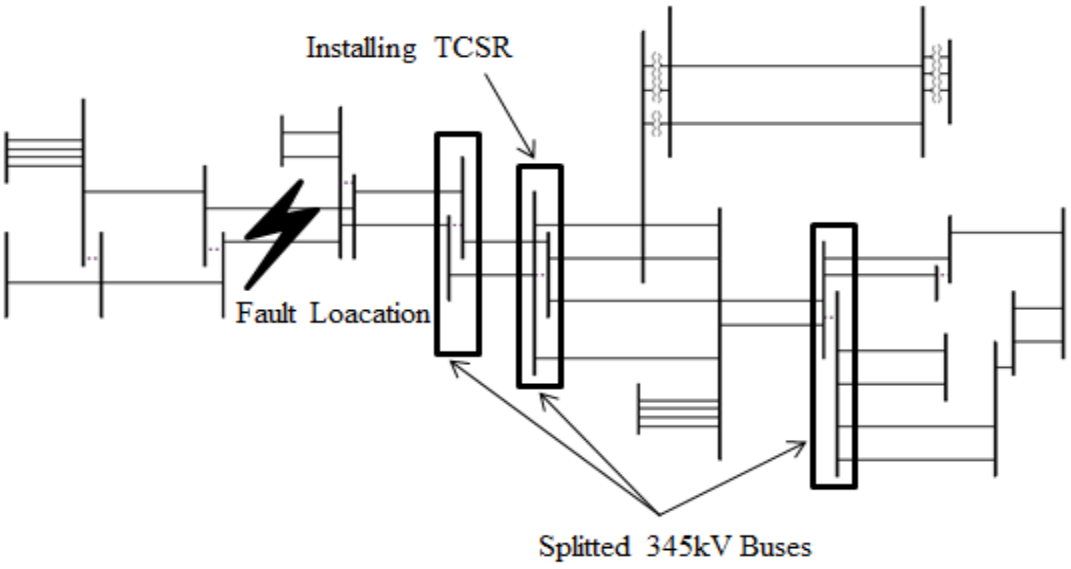

Figure VI.6 A 345kV transmission network for the voltage stability simulation: three substation buses can be reconnected when the TCSR is installed.

To deal with the possible fault currents and voltage stability problems, the network is operated by splitting buses and inter-change flow on some transmission lines is constrained. For the voltage stability assessment, a fault is applied far away from the TCSR. In this case, it does not need to operate as a fault current limiter, because fault currents cannot propagate farther as shown in Table VI.3. It can be seen that the fault currents of other buses far away from 4400 bus are considerably reduced. With the benefit of proposed control actions of the TCSR, we can expect that the voltage will be

maintained higher, and accordingly the voltage stability can be maintained with less dynamic reactive reserves. The interchange flows are increased to 300MW and 475MW, so the available transfer capability of 175MW is achieved. Fault currents are limited within nominal ratings resulting in the reconnection of three split 345kV buses. In addition, this reduces the transmission losses by 3MW at normal operating conditions. The simulation results are summarized in Tables VI.4, VI.5 and Figure VI.7 shows the P-V Curves on a special contingent case.

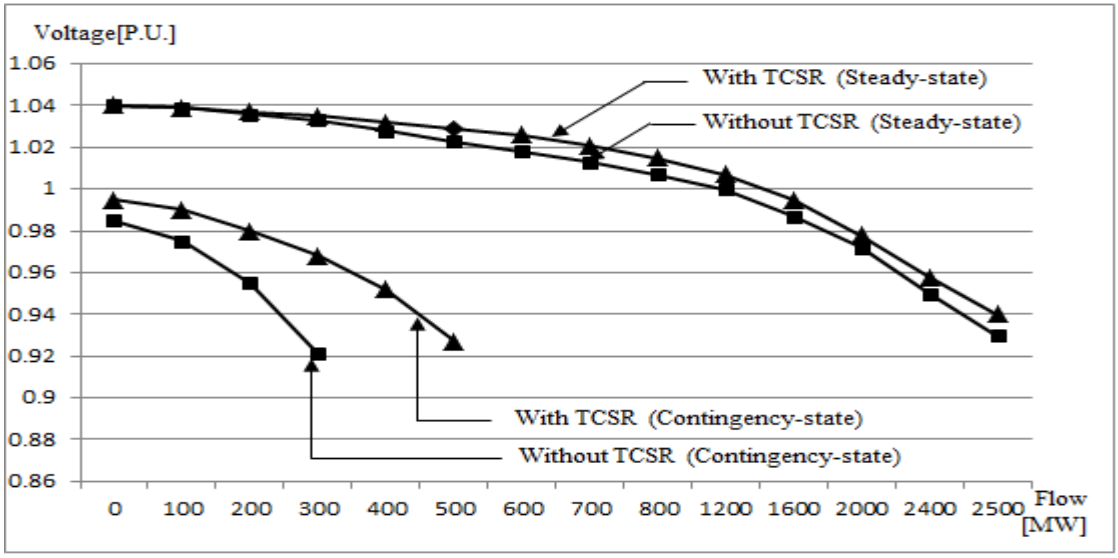

Figure VI.7 P-V curves during normal and contingent conditions: maximum incremental transfer is increased from 300MW to 475MW when the TCSR is used.

Table VI.2 Comparison results of the voltage and the fault current

Fault Location	Condition	Voltage(kV)			Fault Current(kA)
		Prefault	During the fault	Postfault	
FAR	Without TCSR	186.38	148.5	186.38	9.5
	With TCSR	193.9	176.2	193.9	11.2
NEAR	Without TCSR	186.38	0	186.38	37.1
	With TCSR	193.9	0	193.9	38.5

Effects of TCSR on Bulk Power System Angle Stability

On the other hand, if the fault occurs near the place where the TCSR is installed, e.g., a generation site, it should act both as a fault current limiter and a voltage restorer. Fault current limitation and voltage restoration are controlled by a process of changing the impedance of the TCSR, and angle stability is highly related to the impedance behind the machine. Therefore, the power system angle stability can be enhanced by changing the impedance of the TCSR. Based on the concept of Equal Area Criterion [17], power system synchronism can be maintained under the condition where the accelerating power is smaller than the decelerating power.

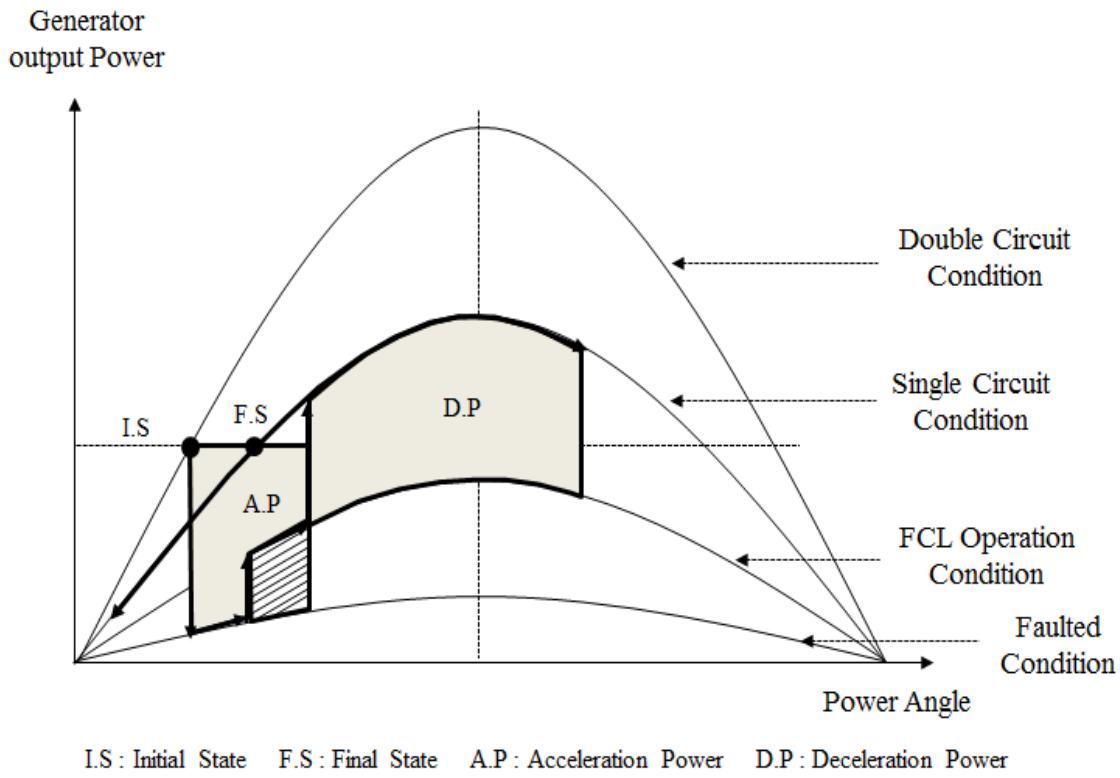

Figure VI.8 Power angle curve for Equal Area Criterion: power system synchronism can be maintained when the accelerating power is smaller than the decelerating power and inserting the series reactor decreases the accelerating power as much as the hatched area.

Considering a Single Machine Infinite Bus (SMIB) system where double circuit transmission line is connected in parallel, network conditions can be represented as: (1) Prefault (both circuits in service), (2) During a three-phase fault, (3) Postfault (circuit 2 out of service) and those are illustrated with P-δ plots in Figure VI.8. When a short-circuit fault occurs, the TCSR reduces the accelerating power as much as the hatched area by inserting the series reactor at the initial stage of the fault.

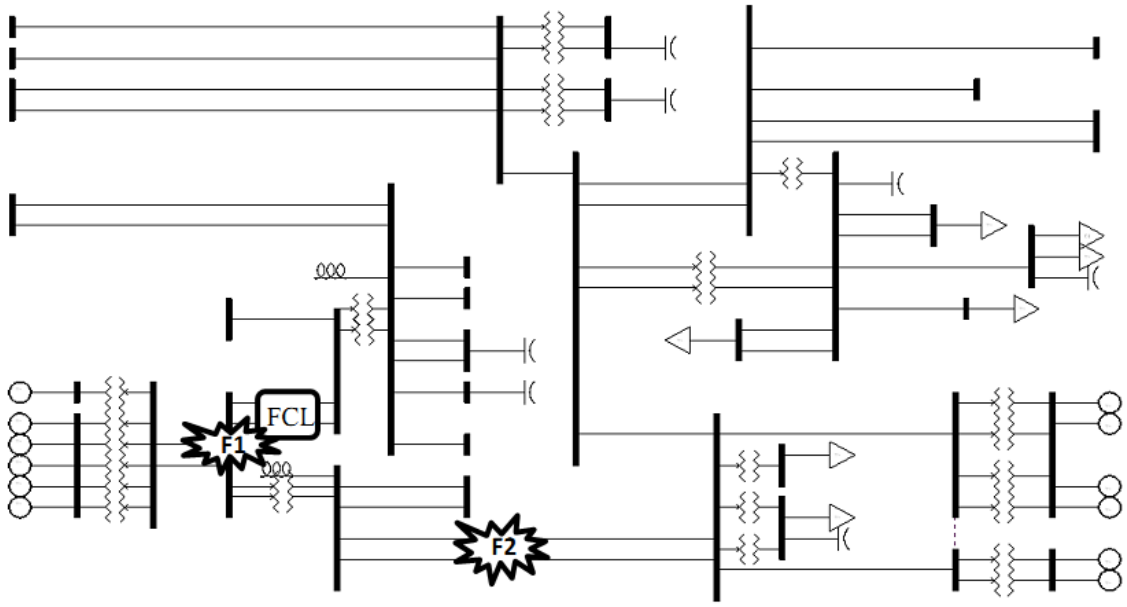

Figure VI.9 Network configuration for the transient stability simulation: a FCL using permanently-inserted series reactor is installed on a substation and two contingency cases (F1, F2) are studied to analyze the influences of the FCL on the power system angle stability.

To assess an impact of the TCSR on the bulk power system angle stability, another fault is applied near the TCSR as shown in Figure VI.9. A permanently inserted series reactor was installed to limit the short-circuit current and a Special Protection Scheme (SPS) such as transfer-trip of some loads and generators, etc. has being applied. In this specific case, simulation shows that the critical clearing time can be increased more than 50msec.

Table VI.3 Fault current of the adjacent buses with respect to 4400 bus fault

Level	Faulted bus / Adjacent bus	4400	4600	6950	2400	4450	2600	3250
0		55.4	49.7	50.5	34.8	34.8	31.0	47.5
1	4600	34.7	15.0					
	6950	29.5		21.0				
2	2400	10.2			24.6			
	4450	16.0				18.8		
3	2600	1.2					29.8	
	3250	17.3						30.2

Table VI.4 Fault current of critical buses(kA)

Bus number	Without TCSR	With TCSR	Rating
1400	43.08	35.34	40
1500	43.94	36.67	40
2500	51.05	48.25	50

Table VI.5 Case summary(MW)

Division	Transmission loss	Max. Incremental Transfer
Without TCSR	1070	300
With TCSR	1067	475

Table VI.6 Critical Clearing Time(msec)

Fault Location	Without TCSR	With TCSR	Difference
F1	70	160	90
F2	50	100	50

Furthermore, considering circuit breaker braking time, we can reduce the number of generators to be tripped when some generators should be tripped with SPS. Figures VI.10, VI.11 and Table VI.6 show the simulation results using PSS/E. With the control action of

the TCSR, the output power of the machine and the system voltage can get to a new stable operating point.

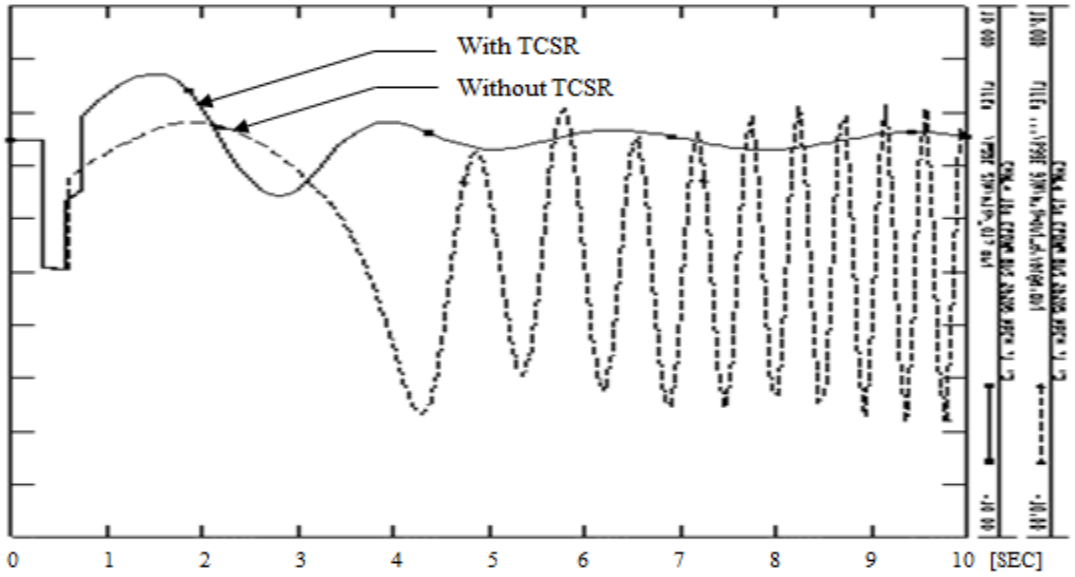

(a)

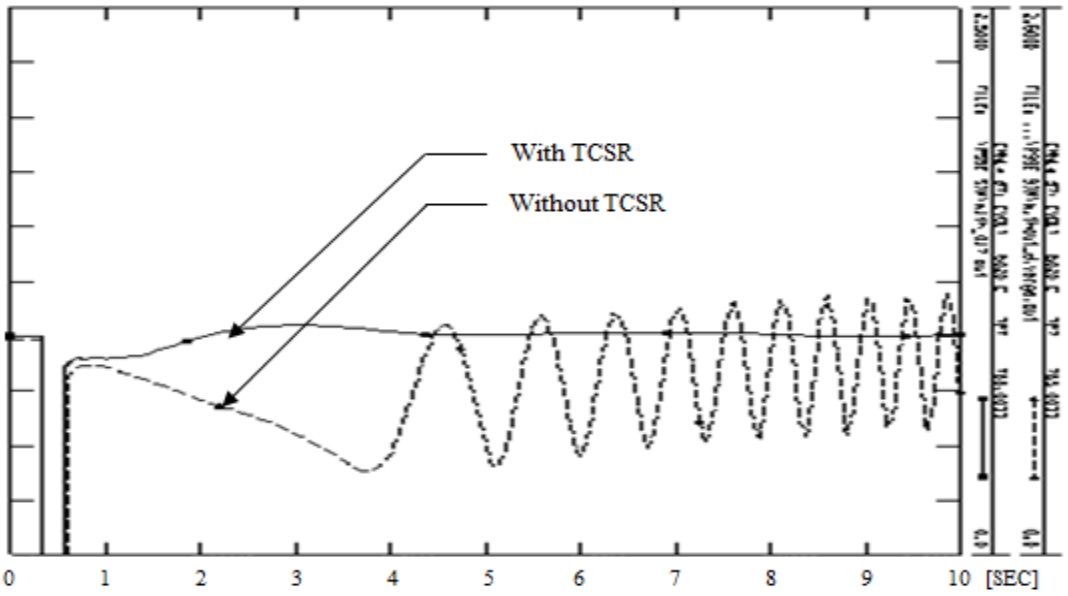

(b)

Figure VI.10 Simulation results on F1 fault: the power system can maintain synchronism with the TCSR (a) Machine electrical power [P.U.] (b) Bus voltage [P.U.].

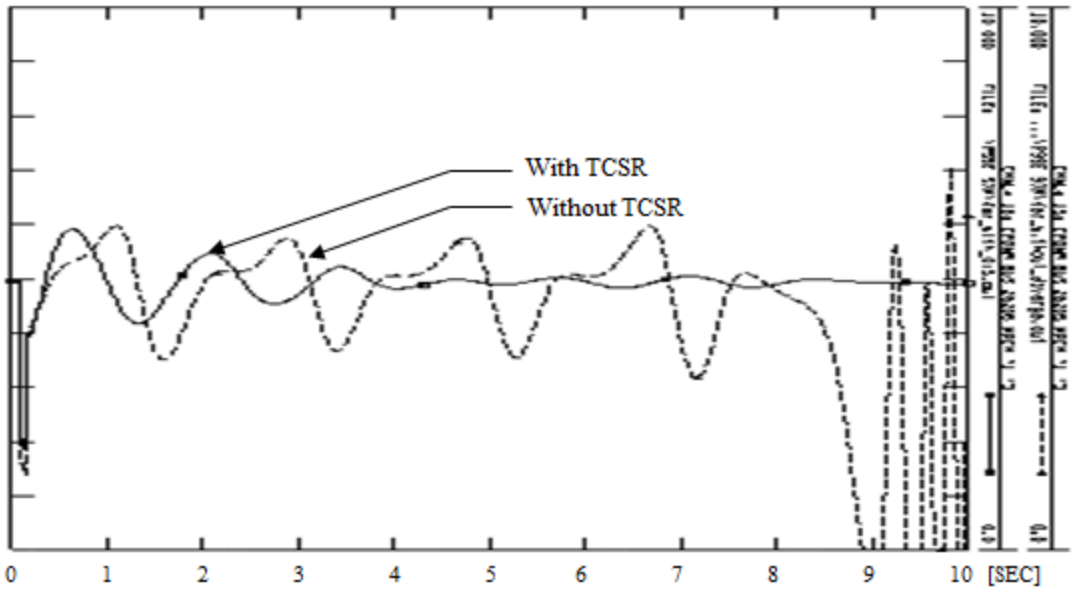

(a)

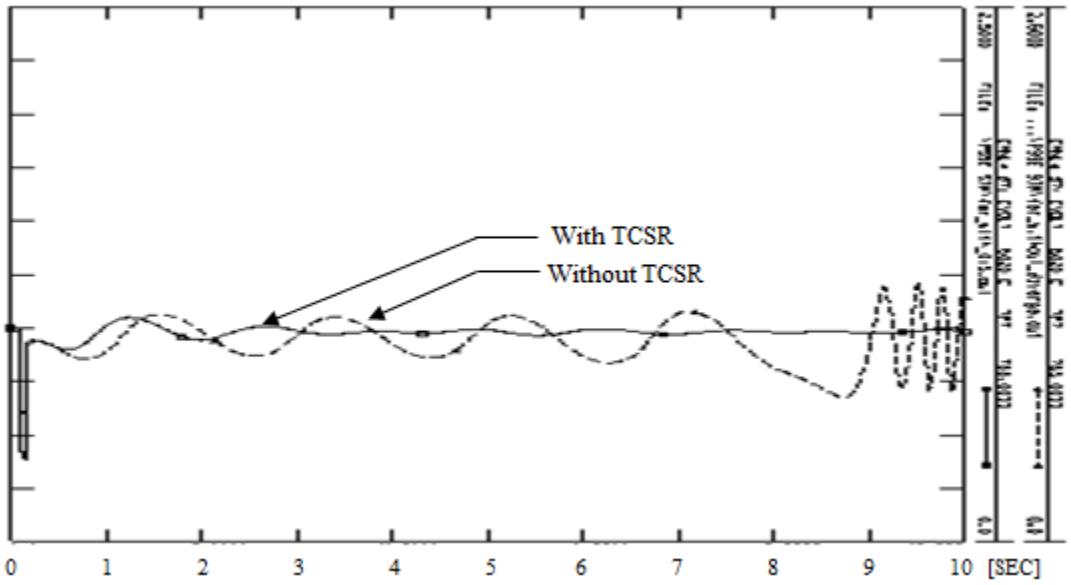

(b)

Figure VI.11 Simulation results on F2 fault: the power system can maintain synchronism with the TCSR (a) Machine electrical power [P.U.] (b) Bus voltage [P.U.].

CHAPTER VII

CONCLUSION

Various kinds of Fault current limiters (FCLs) are being applied in a distribution and transmission network. However, because of the disadvantages on power system operations, such as transmission losses and inferior system stability, their usage has been limited, which has adversely resulted in more investments on constructing transmission lines, replacement of switchgear and degrading the system reliability. However, as the transmission network is meshed and more generations are interconnected to the grid, a capability to deal with both fault current and power system stability is required. This paper has shown that fault currents and stability problems can be managed with the TCSR and a PI controller. It has also been shown that the TCSR can maintain the voltage higher during the fault situation. For the bulk power system, the proposed approach can enhance the system reliability by reducing the number of split buses and increase the available transfer capability and critical clearing time. The validity of the proposed control scheme has been verified with computer simulation using Matlab, PSCAD/EMTDC and PSS/E. The proposed method can be a viable option for the power system planners and operators to make countermeasures to cope with fault current and stability problems.

REFERENCES

[1] O. Mendrock, “Short-circuit current limitation by series reactors," 2009.

[2] V. Tahiliani and J. Porter, “Fault current limiters an overview of epri research," Power Apparatus and Systems, IEEE Transactions on, vol. PAS-99, no. 5, pp. 1964-1969, sept. 1980.

[3] F. Tosato and S. Quaia, “Reducing voltage sags through fault current limitation," Power Delivery, IEEE Transactions on, vol. 16, no. 1, pp. 12-17, jan 2001.

[4] “Proposed terms and denitions for subsynchronous oscillations," Power Apparatus and Systems, IEEE Transactions on, vol. PAS-99, no. 2, pp. 506-511, march 1980.

[5] N. Woodley, L. Morgan, and A. Sundaram, “Experience with an inverter-based dynamic voltage restorer," Power Delivery, IEEE Transactions on, vol. 14, no. 3, pp. 1181-1186, jul 1999.

[6] S. Choi, T. Wang, and D. Vilathgamuwa, “A series compensator with fault current limiting function," Power Delivery, IEEE Transactions on, vol. 20, no. 3, pp. 2248-2256, july 2005.

[7] G. Beck, W. Breuer, D. Povh, and D. Retzmann, “Use of FACTS for system performance improvement," in CEPSI Conference, 2006 Exhibition, November 2006.

[8] A. Abramovitz and K. Smedley, “Survey of solid-state fault current limiters," Power Electronics, IEEE Transactions on, vol. 27, no. 6, pp. 2770-2782, june 2012.

[9] C. Meyer, P. Kollensperger, and R. De Doncker, “Design of a novel low loss fault current limiter for medium-voltage systems, in Applied Power Electronics Conference and Exposition 2004, APEC '04 Nineteenth Annual IEEE, vol. 3, 2004, pp. 1825-1831 Vol.3.

[10] L.Spasojevic, B.Blazic, and I.Papic, “Application of a thyristor-controlled series reactor to reduce arc furnace flicker”, in ELEKTROTEHNISKI VESTNIK 78, 2011, pp. 112-117.

[11] Z.Lu, D.Jiang, and Z.Wu, “A new topology of fault-current limiter and its parameters optimization" in Power Electronics Specialist Conference, 2003, PESC '03, 2003 IEEE 34th Annual, vol. 1, june 2003, pp. 462-465 vol.1.

[12] W. Fei, Y. Zhang, and Z. Lu, “Novel bridge-type fcl based on self-turno devices for three-phase power systems," Power Delivery, IEEE Transactions on, vol. 23, no. 4, pp. 2068-2078, oct. 2008.

[13] A. Fereidouni, B. Vahidi, T. Hoseini Mehr, and M. Garmroodi Doiran, "Enhancement of power system transient stability and power quality using a novel solid-state fault current limiter," Journal of Electrical Engineering & Technology, vol. 6, no. 4, pp. 474-483, 2011.

[14] V. Gor, D. Povh, L. Yichuan, E. Lerch, and D. Retzmann, "SCCL-a new type of FACTS based short-circuit current limiter for application in high-voltage systems," in CIGRE, Session 2004, B4-209, 2004.

[15] S. Sugimoto, J. Kida, H. Arita, C. Fukui, and T. Yamagiwa, "Principle and characteristics of a fault current limiter with series compensation," Power Delivery, IEEE Transactions on, vol. 11, no. 2, pp. 842-847, apr 1996.

[16] J. Dixon, L. Moran, J. Rodriguez, and R. Domke, "Reactive power compensation technologies: State-of-the-art review," Proceedings of the IEEE, vol. 93, no. 12, pp. 2144-2164, dec. 2005.

[17] P.Kundur, "Power system stability and control," 1994.

[18] C.Vatsal, J.Patel, "Simulation and analysis for real and reactive power control with series type FACTS controller," 2012.

[19] D. M. Robert W. Erickson, "Fundamentals of power electronics," 2001.

[20] A. E.N. Gene F.Franklin, J.David Powell, "Feedback control of dynamic systems," 1995.

[21] S.K. Sul, "Control of electric machine drive systems", 2011.